Available online at www.sciencedirect.com

ScienceDirect

Geochimica et Cosmochimica Acta 277 (2020) 265–284

Geochimica et Cosmochimica Acta

www.elsevier.com/locate/gca

Environmental controls on the carbon and water (H and O) isotopes in peatland *Sphagnum* mosses

Zhengyu Xia [a,*], Yinsui Zheng [b], Jonathan M. Stelling [a], Julie Loisel [c], Yongsong Huang [b,*], Zicheng Yu [a,d,*]

[a] *Department of Earth and Environmental Sciences, Lehigh University, Bethlehem, PA, USA*
[b] *Department of Earth, Environmental and Planetary Sciences, Brown University, Providence, RI, USA*
[c] *Department of Geography, Texas A&M University, College Station, TX, USA*
[d] *School of Geographical Sciences, Northeast Normal University, Changchun, China*

Received 2 November 2018; accepted in revised form 24 March 2020; available online 4 April 2020

Abstract

We conducted a modern process study on *Sphagnum magellanicum* from southern Patagonian peat bogs to improve our understanding of environmental controls on the carbon and water (hydrogen and oxygen) isotope compositions of peat mosses. We found that moisture availability gradients in peat bogs, measured by *Sphagnum* water content, could explain the intra-site variability in both *Sphagnum* cellulose $\delta^{13}C$ and $\delta^{18}O$. Also, there was a site-specific significant negative correlation between cellulose $\delta^{13}C$ and $\delta^{18}O$ across microtopographical gradient. This new finding suggests that *Sphagnum* moisture availability influences cellulose $\delta^{13}C$ via water film effect on discrimination against $^{13}CO_2$ and, similarly, can imprint on cellulose $\delta^{18}O$ via evaporative enrichment of ^{18}O in metabolic leaf water. *Sphagnum* leaf wax *n*-alkane $\delta^{13}C$ also responded to the water film effect as cellulose did, but *n*-alkane $\delta^{2}H$ appears less sensitive than cellulose $\delta^{18}O$ to the moisture availability gradient likely because hydrogen isotopes have a more complex biochemical fractionation pathway and a smaller kinetic fractionation during leaf water evaporation. Furthermore, we used long strands of *Sphagnum* to explore if isotopic signals in moss strand increments were sensitive to recent growing season conditions. We demonstrated that rapidly growing *Sphagnum* strand increments could document the isotopic composition of precipitation and moisture conditions at sub-annual scale. Altogether, these findings highlight the sensitivity of stable isotopes in *Sphagnum* to environmental conditions. On the basis of these results, we propose that paired measurements of carbon and water isotopes in *Sphagnum* cellulose or leaf wax biomarker provide an improved approach in peat-based paleoclimate reconstructions.

Keywords: Sphagnum; peatland; stable isotopes; plant physiology; water content

1. INTRODUCTION

Peatland ecosystems—occupying only 3% of the global land area—are terrestrial carbon hot spots that have sequestered over 600 gigatons of organic carbon since the Last Glacial Maximum (ca. 21,000 years before present; Yu et al., 2010). Paleoenvironmental analysis using peat deposits provides valuable insights into peatland evolution, ecosystem dynamics, and past climate conditions. A range

* Corresponding authors at: Department of Earth and Environmental Sciences, Lehigh University, Bethlehem, PA, USA (Z. Xia and Z. Yu); Department of Earth, Environmental and Planetary Sciences, Brown University, RI, USA (Y. Huang).
E-mail addresses: zhx215@lehigh.edu (Z. Xia), yongsong_huang@brown.edu (Y. Huang), ziy2@lehigh.edu (Z. Yu).

https://doi.org/10.1016/j.gca.2020.03.034
0016-7037/

of proxy-climate indicators, including bulk density, humification, testate amoebae, charcoal, and plant macrofossils, have been routinely used in peat-based paleoenvironmental reconstructions (e.g., Woodland et al., 1998; Barber et al., 2000; Turney et al., 2004). Stable isotope proxies from peat-forming plant remains are important supplements to the more classic peat-core analysis toolbox (Brenninkmeijer et al., 1982; Chambers et al., 2012). *Sphagnum* mosses are a group of remarkable peat-forming plants as the main "peat builder" that possess many unique physiological characteristics and are resistant to microbial breakdown (Rydin and Jeglum, 2013). Also known as peat mosses, *Sphagnum* have attracted the most attention in exploring the potential of their stable isotope compositions as paleoenvironmental proxies (e.g., Xie et al., 2000; Ménot and Burns, 2001; Ménot-Combes et al., 2002; Xie et al., 2004; Daley et al., 2010; Nichols et al., 2010; Nichols et al., 2014; Granath et al., 2018). Understanding the physiological process mechanisms underlying the isotopic variations in modern *Sphagnum* plants is required for robust environmental interpretations of long-term isotopic variations preserved in *Sphagnum* peat records.

Carbon isotope signatures ($\delta^{13}C$) in *Sphagnum* follow the general carbon isotope fractionation model for C3 plants that considers kinetic isotope effects in CO_2 diffusion and carboxylation (Farquhar et al., 1989). The model has been further adapted for mosses that lack stomata and have an external water film on outer surface (Meyer et al., 2008; Royles et al., 2012). Royles et al. (2012) showed that several factors can affect carbon isotope discrimination, but CO_2 assimilation rate is the dominant factor for aerobic (non-waterlogged) peatbank moss species in maritime Antarctic. In their theoretical study, mosses only attain external water film after a rain or snow melt event but then dry out quickly. In contrast, *Sphagnum* mosses often inhabit waterlogged peatlands and have great water retention capacity with a persistent external water film. As a result, moisture regime affects both *Sphagnum* CO_2 assimilation rate and carbon isotope fractionation caused by diffusion resistance, as CO_2 diffusivity is much lower in water than in air (Rice and Giles, 1996; Rice, 2000). Empirical studies supported that moisture availability exerts a major control on *Sphagnum* $\delta^{13}C$ known as the water film effect (Price et al., 1997; Ménot and Burns, 2001; Loisel et al., 2009; Loader et al., 2016): drier *Sphagnum* mosses are characterized by thinner water films that have less diffusion resistance and result in more discrimination against $^{13}CO_2$, leading to more negative $\delta^{13}C$ values in plant tissues, and vice versa. This effect is expressed at microtopographical gradients (e.g., hummock vs. hollow) within a peatland. A few additional factors were also shown to affect peatland *Sphagnum* $\delta^{13}C$, which include (1) the contribution of recycled CO_2 (Price et al., 1997), in particular the methane-derived CO_2 that is strongly depleted in ^{13}C and is efficiently fixed by *Sphagnum* in wet habitats (Raghoebarsing et al., 2005; Nichols et al., 2009; Nichols et al., 2014); and (2) air temperature, although both positive and negative correlations between temperature and *Sphagnum* $\delta^{13}C$ have been reported in the literature (Skrzypek et al., 2007; Kaislahti Tillman et al., 2013). Therefore, *Sphagnum* cellulose and leaf wax $\delta^{13}C$ have been used to reconstruct past temperature and hydroclimate changes from peat records, often with contrasting interpretations (Xie et al., 2004; Nichols et al., 2009; Loisel et al., 2010; Moschen et al., 2011; Kaislahti Tillman et al., 2013).

For ombrotrophic (rain-fed) peat bogs, water (hydrogen and oxygen) isotope signatures in *Sphagnum* are determined by the isotopic composition of precipitation, subsequent evaporative enrichment of ^{18}O and ^{2}H in leaf water, and biochemical fractionation. The fractionation process in cellulose biosynthesis has been shown to follow the form of (Anderson et al., 2002; Zanazzi and Mora, 2005; Daley et al., 2010):

$$\delta^{18}O_{cell} = \delta^{18}O_p + \varepsilon_b + (\varepsilon_e + \varepsilon_k)(1 - h) \quad (1)$$

where $\delta^{18}O_{cell}$ and $\delta^{18}O_p$ are the oxygen isotope composition of cellulose and precipitation, respectively; ε_b is the biochemical enrichment factor during cellulose biosynthesis; ε_e and ε_k are liquid–vapor equilibrium and kinetic enrichment factor associated with leaf water evaporation, respectively; and h is the relative humidity. It was argued that the evaporation term in Eq. (1) could be removed, because *Sphagnum* mosses lack stomata and inhabit moist environments with h close to 100% (Zanazzi and Mora, 2005; Daley et al., 2010). If assuming that biochemical fractionation term ε_b is a stationary value over time, then *Sphagnum* cellulose $\delta^{18}O$ and $\delta^{2}H$ as well as leaf wax $\delta^{2}H$ can be used to infer the isotopic compositions of past precipitation, which provide information about large-scale macroclimate drivers such as air temperature, precipitation sources, and atmospheric circulation patterns (Xie et al., 2000; Pendall et al., 2001; Daley et al., 2009; Daley et al., 2010; Bilali et al., 2013; Xia et al., 2018). However, the model given above have two deficiencies that need to be considered when applied to mosses. First, Eq. (1) was based on the Craig–Gordon model (Craig and Gordon, 1965) that depicted leaf water evapotranspiration through stomata as an analogue to steady-state evaporation of a closed lake (Ménot-Combes et al., 2002). It considered leaf water exchange with ambient water vapor through stomata and assumed that all leaf water was subject to evaporation (Anderson et al., 2002). It might be inappropriate to apply Eq. (1) to *Sphagnum* mosses, which lack stomata and evaporate leaf water through tiny pores on water-reservoir hyaline cells, preventing liquid-vapor interaction (Nichols et al., 2010). Second, the assumption of no evaporation with h at 100% is not always justified, as it would predict that $\delta^{18}O_{cell}$ values were conservative and independent from microhabitat within a peatland. This is in contradiction with empirical evidence showing that *Sphagnum* leaf water is more enriched in ^{18}O and ^{2}H than meteoric water input and there is a clear hydrogen and oxygen isotope variability in *Sphagnum* tissues explained by differential degree of evaporative enrichment at microtopographical scale (Aravena and Warner, 1992; Ménot-Combes et al., 2002; Zanazzi and Mora, 2005; Nichols et al., 2010; Loader et al., 2016).

Our understanding of environmental controls on the carbon and water (H and O) isotope variability in *Sphagnum* tissues has improved in recent years, but a coherent

physiological interpretation is not achieved. Still, most peat-core studies that undertook stable isotope analyses only utilized a single isotope proxy, such that the investigators were unable to examine the intrinsic relationships between the carbon and water (H and O) isotope ratios in *Sphagnum* organic compounds. Without a multi-proxy framework, it can be challenging to reconcile the multiple controlling factors on *Sphagnum* isotope ratios for paleoenvironmental interpretations, particularly for the relative role of evaporative enrichment on water isotope proxies (Daley et al., 2009; Finkenbinder et al., 2016). Given that moisture availability influences *Sphagnum* carbon isotope signatures via the water film effect, and that the degree of evaporative enrichment of ^{18}O and ^{2}H in leaf water also depends on moisture availability that is highly variable at microtopographical scale, there should be a negative correlation between these two isotope ratios. Demonstrating this carbon–water isotopic link in modern *Sphagnum* samples would provide a useful means to properly interpret peat-based climate-proxy records with a "dual isotopes" approach (Roland et al., 2015; Xia et al., 2018).

Here we present a dataset of paired cellulose $\delta^{13}C$ and $\delta^{18}O$ measurements of modern *Sphagnum magellanicum* from southern Patagonian peat bogs. Plant and leaf water samples were collected along a wide range of habitats and moisture gradients across multiple sites. We measured the water content (WC; the ratio of mass between water and dry plants) of each *Sphagnum* sample as an independent indicator of *Sphagnum* moisture availability, in an attempt to explore how moisture availability influences cellulose $\delta^{13}C$ and $\delta^{18}O$ concurrently. We also present data from *Sphagnum* leaf wax biomarker *n*-alkane $\delta^{13}C$ and $\delta^{2}H$ measurements to test the same hypothesis. Furthermore, our previous work found that *S. magellanicum* in southern Patagonian peat bogs were growing fast and formed long strands that could reach over 45 cm in length, and indeed these peatlands had rapid accumulation rates due to enhanced *Sphagnum* growth (Loisel and Yu, 2013a; Loisel and Yu, 2013b). As an extreme example, a Patagonian peatland has accumulated over 300 cm of *Sphagnum* peat in less than 500 years, which is an order of magnitude faster than boreal peatlands (Loisel and Yu, 2013a; Loisel and Yu, 2013b). Therefore, we additionally explored if isotopic signals in *Sphagnum* strand increments could document recent growing season conditions at sub-annual scale, including monthly and seasonal changes in isotopic composition of precipitation and precipitation anomalies, to understand the nature and sensitivity of *Sphagnum* isotopic signals preserved in peat records. With this new understanding of *Sphagnum* isotopic physiology, we then further discussed the potential of using paired carbon and water (H or O) isotope measurements in peat-core analysis for paleoclimate reconstructions.

2. METHODS

2.1. Study sites and sample collections

Southern Patagonia is characterized by a large precipitation gradient driven by interactions between strong westerly winds and north-south oriented mountain ranges of the Andes. Despite the widespread distribution of peatlands in Patagonia (Fig. 1), *Sphagnum*-dominated peat bogs are only present on the eastern side (leeward side) of the Andes, where annual precipitation amounts are generally between 400 and 1000 mm (Loisel and Yu, 2013a). *Sphagnum magellanicum* is the dominant species in these peat bogs, forming large carpets that cover a vast peatland complex (Fig. 2). Field sampling was carried out at six sites in January 2016 and another site (Ariel Peatland) in January 2018 (Table 1). These sites are located between 52.1°S and 54.5°S and between 68.7°W and 71.9°W (Fig. 1). High-resolution (5.5 km) regional climate modeling (Lenaerts et al., 2014) indicates an existing climate gradient (precipitation in particular) across these sites (Table 1), but more importantly these peatlands differ in hydromorphological characteristics (Fig. 2). According to Rydin and Jeglum (2013), *hydromorphology* is a term used to express interactions between biotic and abiotic factors that shape the surface morphology and patterning of peatlands. As described below, our sampling strategy was designed to capture the greatest local moisture gradient of *Sphagnum* habitat within each site.

2.1.1. Surface Sphagnum

Our first site, Valle de Consejo (VC), is characterized by well-developed hummock-hollow-pool surface patterning. We established a 450-cm sampling transect along a large hummock-to-pool gradient (north-facing) with a relative relief of ~70 cm (Fig. 2a and b). The entire gradient was mainly colonized by *S. magellanicum*. Another species (*S. cuspidatum*) was found on the edge of the open-water pool (Fig. 2b). We collected surface samples (top ~3 cm) of living *Sphagnum* at 30-cm intervals from the hummock top down to the pool, with an additional sample at the boundary between the two *Sphagnum* species (n = 17, including three *S. cuspidatum* samples). We collected duplicate samples that were kept in sealable bags for subsequent water content (WC) measurements in the laboratory. We also measured *in situ* water table depth (WTD) at some sampling locations along the transect by digging small pits with a peat borer. Similarly, a 250-cm transect was sampled across a northeast-facing hummock-to-hollow gradient at Villa Runeval (VR) with a relative relief of ~60 cm. This site, which was only sampled for *S. magellanicum* (n = 5), is characterized by very dry bog surface (Fig. 2c). WC samples were collected for this site, but *in situ* WTD was not measured.

The Ariel Peatland (AP) has less pronounced microtopographical structures with a relatively flat and moist peatland surface at the center (Fig. 2d and e). The sampled moisture gradient thus extended from the peatland's edge, where dry-adapted shrubs were found, to the center of the site, where *S. magellanicum* was abundant. We collected nine evenly distributed *S. magellanicum* samples across this peatland-wide moisture gradient. Similarly, site Cordillera Chilena (CC) is a high-elevation slope bog (Fig. 2f and g), where we collected six *S. magellanicum* samples along the slope (with an elevation difference of ~20 m) following the same sampling strategy as for site AP. Lastly, oppor-

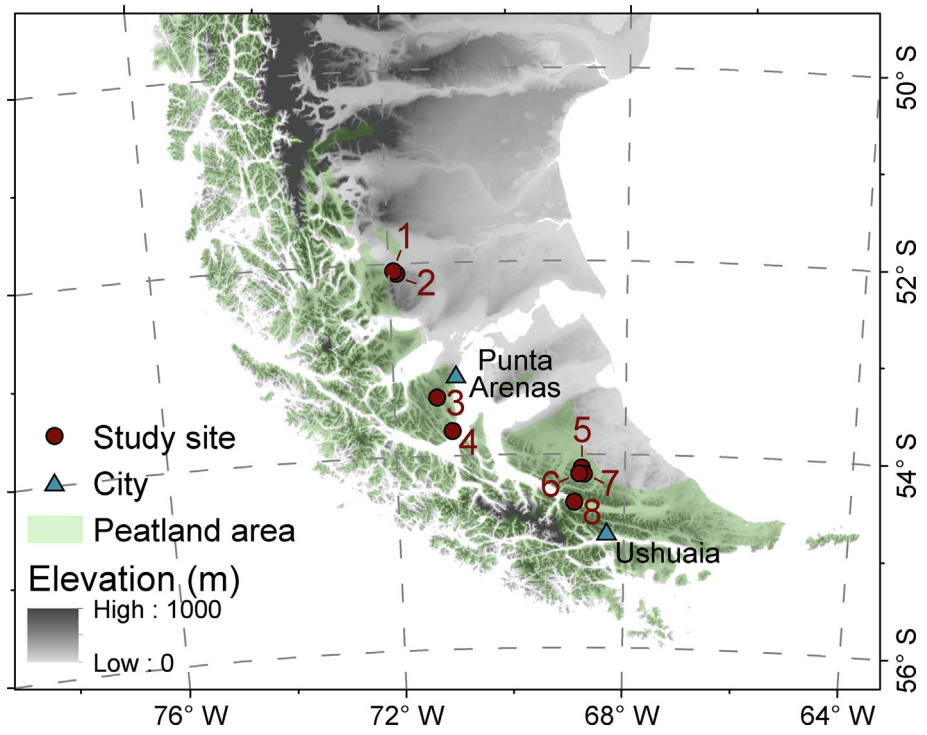

Fig. 1. Map of southern Patagonia shown with digital elevation model and study site locations. The extent of peatland-dominated area (peatland covering at least 5% of landmass) is based on Yu et al. (2010). Dark red circles show peatland sites discussed in this study: 1–Villa Runeval (VR), 2–Cordillera Chilena (CC), 3–Laguna Parrillar (LP; Loader et al., 2016), 4–Monte Tarn (MT), 5–Mirador Laguna Cura (MLC), 6–Valle de Consejo (VC), 7–Ariel Peatland (AP), 8–Azopardo (AZ). The sites VR and CC are in the Laguna Blanca region, and the sites MLC, VC, and AP are in the Karukinka Park region. Blue triangles also show major cities in this region where the Global Network of Isotopes in Precipitation (GNIP) data are available. (For interpretation of the references to color in this figure legend, the reader is referred to the web version of this article.)

tunistic *S. magellanicum* samples were collected at three additional sites: (1) six samples from site Monte Tarn (MT), which is a wooded bog developing on a mountain slope where vegetation changes from forest to tundra within a 600-m elevation increase with *Sphagnum* widely present along a hiking trail (Fig. 2h and i); (2) two samples from site Mirador Laguna Cura (MLC); and (3) two samples from site Azopardo (AZ). Again, for all these samples, duplicate WC samples were also collected.

2.1.2. Plant water and bog water sampling

During surface *Sphagnum* sampling, each of the same living plants were immediately squeezed using a syringe to collect "bulk" leaf water into 2 mL vials in the field. Opportunistic bog water samples were collected at site VC, AP, and CC, after small pits were dug using a peat borer at the exact location where surface *Sphagnum* was sampled.

2.1.3. Sphagnum strands

At site CC and VC, we found that *Sphagnum* often maintained >20 cm long intact strands that likely indicated rapid growth over the course of recent growing seasons (Fig. 3). Similar long strands were also found at some sites in our previous field excursion in southern Patagonia (Loisel and Yu, 2013a). We collected the uppermost section of peat as a monolith from both sites that contained those long strands of *Sphagnum*, which were individually extracted and further subsampled in the laboratory.

2.2. Laboratory analysis

2.2.1. Water content measurements

Samples for water content (WC) measurements were dried in an oven at 50 °C overnight. The sample weights before and after oven drying were measured. The WC was calculated as (Rydin and McDonald, 1985; Murray et al., 1989; Schipperges and Rydin, 1998):

$$\mathrm{WC}\ (\%) = \frac{m_w - m_d}{m_d} \times 100 \qquad (2)$$

where m_w and m_d are the wet weight and dry weight, respectively. Note that a few studies defined the metric using the same formula as relative water content (RWC) (e.g., Royles et al., 2013a, 2013b), which is a term originally defined as the ratio of the amount of water in the leaf tissue to that present when fully turgid (Smart and Bingham, 1974). Despite being applied to vascular plants, the RWC is not easy to determine for bryophytes due to the difficulty to estimate turgid weight (Dilks and Proctor, 1979). Furthermore, other studies defined the ratio of wet weight to dry

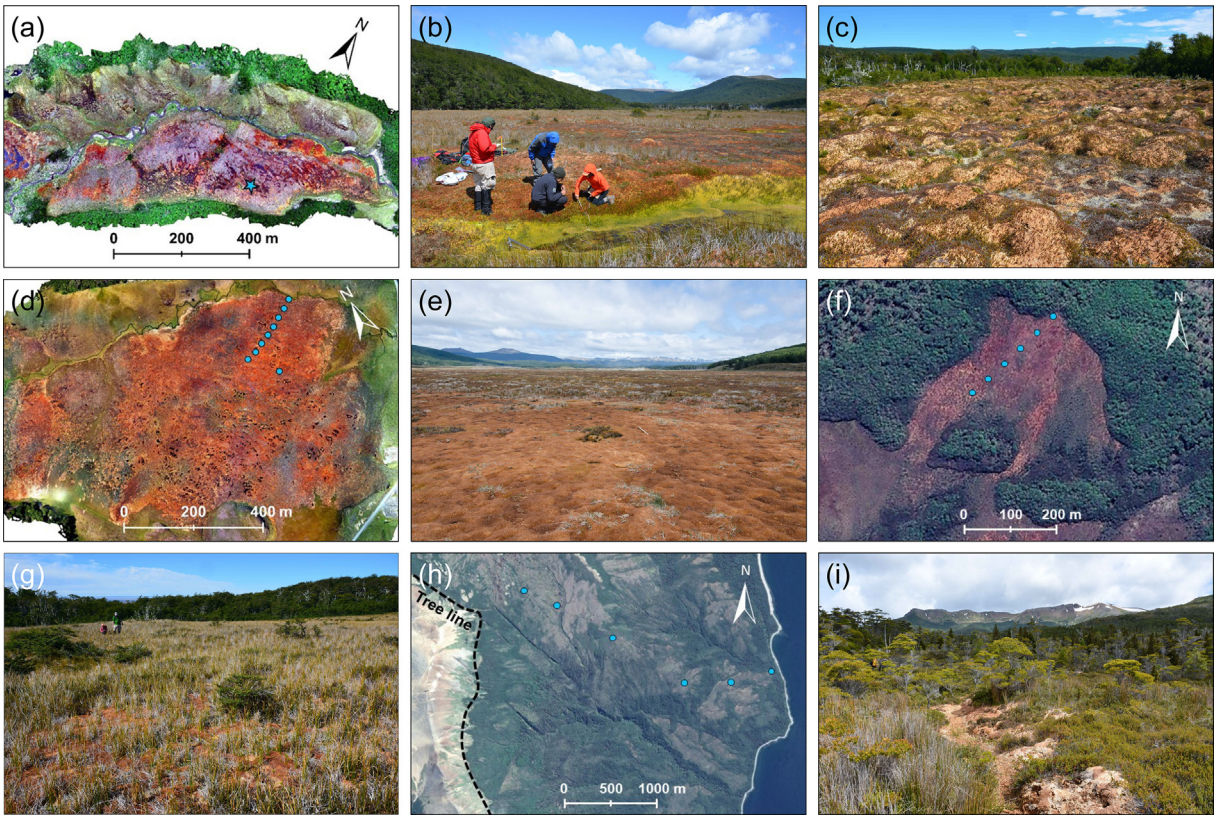

Fig. 2. Aerial and ground photos showing diverse peatland hydromorphology. (a, b) Site VC, a raised and patterned bog where a large hummock-to-pool transect was sampled with its location shown as blue star in aerial view. (c) Ground photo of site VR, a very dry bog with hummock-hollow patterning. (d, e) Site AP, an open bog with relatively flat bog surface with its center dominated by pure *Sphagnum* carpets. (f, g) Site CC, a high-elevation bog on a gentle slope. (h, i) Site MT, a wooded bog with *Sphagnum* covering vast blanket on a mountain slope, with treeline outlined on aerial view (dashed line). Filled blue symbols in some aerial photos indicate the locations of surface *Sphagnum* samples collected with a goal to capture intra-site moisture gradient. All ground photos were taken by Z. Yu. Aerial photos were taken on an unoccupied aerial vehicle (drone) by J. M. Stelling (a, d) or derived from Google Earth imagery (f, h). (For interpretation of the references to color in this figure legend, the reader is referred to the web version of this article.)

weight as WC (e.g., Titus et al., 1983; Titus and Wagner, 1984).

2.2.2. Surface Sphagnum subsampling

To prepare cellulose samples, surface *Sphagnum* samples (n = 47 in total) were examined under a stereomicroscope to make sure that only the topmost 1-cm sections of stem below the *Sphagnum* capitulum, which represented the most recent growth, were used for cellulose extraction. For each subsample, around 15 individual stems were combined. Other moss components (leaves, branches, and older stems) were removed. The reason for restricting our analysis on stem tissues is to make our pre-treatment procedure and cellulose isotopic signatures comparable with peat-core studies, in which *Sphagnum* stem macrofossils could easily be collected to sufficient amount (Xia et al., 2018), and to avoid mixture of different tissues that showed somewhat isotopic offsets (Loader et al., 2007; Moschen et al., 2009; Kaislahti Tillman et al., 2010).

To prepare leaf wax samples, we just used bulk *Sphagnum* capitula (~0.6 g dry wt.) from selective samples for lipid extraction. For site VC, we analyzed seven samples. For other sites, we analyzed only one sample from each site.

2.2.3. Sphagnum strand subsampling

For *Sphagnum* strand samples, we noticed that stem bifurcations or innovation formations were quite frequent as a result of vegetative reproduction, but new bifurcated strands showed similar length with their siblings (Fig. 3c). To prepare cellulose samples, we picked out one individual *Sphagnum* strand that possessed multiple bifurcations from the CC monolith, cut it into 1-cm sections, and combined corresponding sections from bifurcated strands to generate enough materials for cellulose extraction. We had to assume that bifurcated strands had similar incremental rate. We followed the same procedure for one strand from the VC monolith, but they were cut into 2-cm sections. The sectioned samples were then examined under a stereomicroscope to isolate stem tissues for cellulose extraction.

Among the individual *Sphagnum* strands, we observed that the stem bifurcations were roughly consistent with an occurrence rhythm of ~7 cm, likely indicating similar

Table 1
Summary information for study sites and their peatland hydromorphology descriptions.

Site number[a]	Site name	Latitude (° S)	Longitude (° W)	Elevation (m)	MAT[b] (° C)	MAP[b] (mm)	MRH[b] (%)	Peatland area (km^2)	Hydromorphological features
1	Villa Runeval (VR)	52.08	71.92	262	3.8	1735	81	0.2	Very dry bog with hummock-hollow patterning
2	Cordillera Chilena (CC)	52.10	71.87	514–533	3.9	1475	80	0.3	High-elevation bog on hillslope
3	Laguna Parrillar (LP)[c]	53.40	71.25	309	3.7	742	80	2.9	Large open bog with dense vascular plant cover
4	Monte Tarn (MT)	53.75	71.00	24–503	3.4	2004	81	>3	Wooded bog with *Sphagnum* covering vast blanket on mountain slope
5	Mirador Laguna Cura (MLC)	54.14	68.75	391	8.0	762	76	0.06	Small bog localized on foothill surrounded by forested area
6	Valle de Consejo (VC)	54.21	68.79	229	7.9	850	78	0.2	Raised bog with significant hummock-hollow-pool patterning
7	Ariel Peatland (AP)	54.21	68.72	165	7.9	686	75	0.7	Open bog with flat surface and concentric vegetation zonation, with bog center occupied by solely *Sphagnum*
8	Azopardo (AZ)	54.50	68.88	55–110	2.6	1132	81	>2	Blanket bog on hillslope on both sides of paved road

[a] These are site numbers shown in Fig. 1.
[b] Gridded mean annual temperature (MAT), mean annual precipitation (MAP) and mean annual relative humidity (MRH) data are from output of high-resolution (5.5 km) regional climate model applied to Patagonia and driven by the European Centre for Medium-Range Weather Forecasts (ECMWF) ERA-Interim reanalysis during AD 1979–2012 (Lenaerts et al., 2014).
[c] Site reported by Loader et al. (2016).

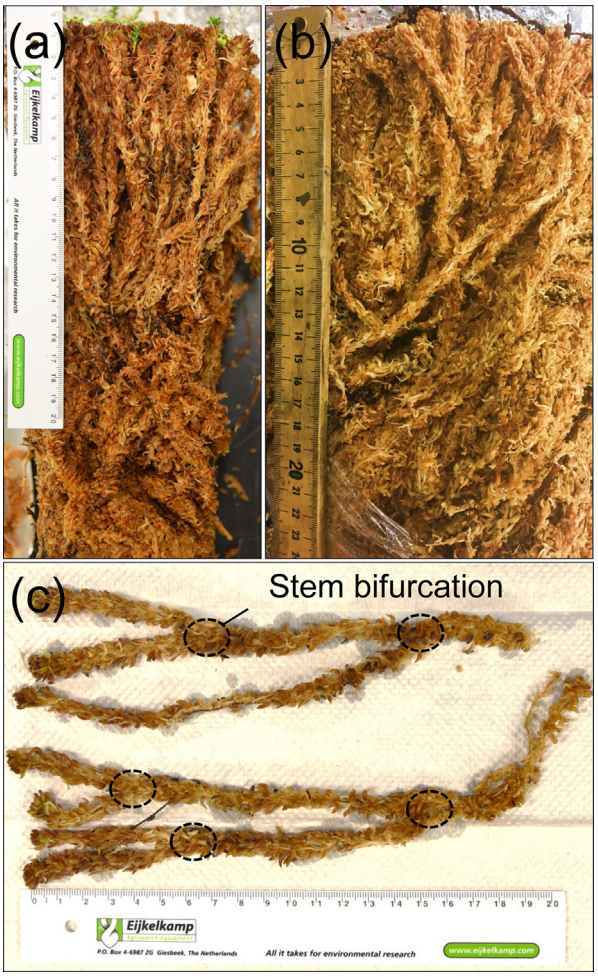

Fig. 3. Photos of (a) monolith from site CC and (b) monolith from site VC. (c) Photo shows that long *Sphagnum* strands extracted from monolith CC were lined up for subsampling on stem increments for isotope analysis. Position of stem bifurcation are marked.

growth rate even among multiple individuals (Fig. 3c). Although there are very few studies on *Sphagnum* stem bifurcations (Sobotka, 1976), we tested the hypothesis that bifurcations could be used as a roughly time marker by lining up 18 individuals picked out from the CC monolith and comparing the occurrences of stem bifurcations along the *Sphagnum* strands. Then we selected the 10 *Sphagnum* individuals with the highest bifurcation match, cut them into 1-cm sections, and combined them to generate enough materials for lipid extraction (~0.25 g dry wt.). We analyzed seven sectioned strand samples at 2-cm intervals.

2.2.4. Cellulose isotope analysis

The method of cellulose extraction followed the alkaline bleaching method (Kaislahti Tillman et al., 2010). Stem collections were transferred to disposable polypropylene columns (Poly-Prep). Samples were subjected to 5 rounds of 1.4% (w/v) sodium chlorite bleaching acidified with glacial acetic acid in a hot water bath at 80 °C, each round for 50 min. Then, they were reacted with 10% (w/v) sodium hydroxide at 75 °C for 45 min and another 2 rounds of acidified sodium chlorite bleaching. The yielded α-cellulose was rinsed with distilled deionized water and transferred to small vials. Afterwards, samples were homogenized using an ultrasonic probe and freeze-dried.

For oxygen and carbon isotope analysis, ~0.4 mg and ~1.1 mg cellulose materials were enclosed in silver and tin capsules, respectively. Strand subsamples were small in sample size, thus only ~0.25 mg and ~0.5 mg materials were used. Oxygen isotope compositions were determined on an Elementar PyroCube interfaced to an Isoprime VisION isotope-ratio mass spectrometer (IRMS). Carbon isotope compositions were determined on a PDZ Europa ANCA-GSL elemental analyzer interfaced to a PDZ Europa 20–20 IRMS. Both isotopic analyses were carried out at the Stable Isotope Facility (SIF) of University of California, Davis. By convention, results of isotope ratio measurements were reported as δ notation (in per mille) referenced to VPDB (Vienna Pee Dee Belemnite) for $\delta^{13}C$ and to VSMOW (Vienna Standard Mean Ocean Water) for $\delta^{18}O$. During analysis, samples were interspersed with replicates of established calibration standards and several check standards with known isotopic compositions. The check standards were used to monitor the analytical drift and size effect and corrections were applied when necessary to ensure analytical accuracy for sample measurements. Precision of measurements was assessed by standard deviation (1σ) of replicate analyses of standards, which was less than 0.09‰ for $\delta^{13}C$ and 0.22‰ for $\delta^{18}O$. The standard deviation (1σ) of replicate analyses of samples for $\delta^{18}O$ was less than 0.21‰, suggesting our cellulose samples were well homogenized.

2.2.5. Leaf wax isotope analysis

Prepared leaf wax samples were washed, freeze dried, and extracted for lipids using a Dionex Accelerated Solvent Extractor (ASE) with a 9:1 (v/v) solution of dichloromethane and methanol at 120 °C and 1200 psi. The total lipid extracts were separated over flash column chromatography with silica gel (40–63 μm, 60 Å), and the *n*-alkanes were eluted with hexane. Concentrations of *n*-alkane compounds were determined on an Agilent 6890 gas chromatography-flame ionization detector (GC-FID), with an internal standard (hexamethylbenzene) added into each sample vial. The *n*-alkane compounds were identified by comparing the retention times with a mixture of external *n*-alkane standards (C_{25}, C_{27}, C_{29}, C_{30}, and C_{32} *n*-alkane). Compound-specific carbon isotope ratios and hydrogen isotope ratios for *n*-alkanes were determined on an Agilent HP-6890 gas chromatograph (GC) interfaced to a Thermo Finnigan Delta + XL stable isotope ratio mass spectrometry (IRMS) through a high-temperature pyrolysis reactor. Both GC-FID and GC-IRMS analyses were carried out at Brown University. Detailed information about analytical methods could be found in Li et al. (2018). The compound-specific *n*-alkane $\delta^{13}C$ (referenced to VPDB) were measured once or twice, while $\delta^{2}H$ (referenced to VSMOW) were measured in triplicate with means and standard deviations (1σ) determined. External standard mixture was also interspersed and measured throughout to monitor instrument

performance. The isotopic compositions of these laboratory standards were established by repeated measurements after verifying the instrument performance using the standard compounds acquired from Indiana University. The offsets between measured and established δ^2H values for laboratory standards during analyses of individual sample batches can range from 3 to 7‰. The offsets were used to correct sample δ^2H on daily batches and ensure accuracy. Correction was not needed for sample $\delta^{13}C$ as the offsets were very small (less than 0.1‰). The overall analytical precision was assessed using pooled standard deviation (1σ) of replicate analyses of standards or samples (C_{21}, C_{23}, and C_{25} *n*-alkane only) following Daniels et al. (2017), which was less than 0.23‰ for $\delta^{13}C$ and 3.14‰ for δ^2H.

2.2.6. Water sample isotope analysis

The squeezed leaf water and bog water samples were treated with activated charcoal and filtered to remove dissolved organic matter before being analyzed for hydrogen and oxygen isotope compositions using a Picarro model L1102-i isotopic liquid water and water vapor analyzer at Brown University. Samples were analyzed with Picarro ChemCorrect software and no sample was flagged as being contaminated. Each sample was measured in eight injections and the first two injections were discarded for between-sample memory. Four secondary isotopic standards were established by directly being calibrated against primary isotopic standards (VSMOW, USGS-46, and USGS-49). Accuracy was assessed by interspersing these secondary isotopic standards throughout samples and comparing their measured values with established values. The offset was less than 0.43‰ for δ^2H and 0.22‰ for $\delta^{18}O$. The overall analytical precision was assessed using pooled standard deviation (1σ) of replicate analyses of samples, which was 0.61‰ for δ^2H and 0.10‰ for $\delta^{18}O$.

2.3. Statistical analysis

To statistically test the correlation among isotope data and WC measurements, we performed the Pearson correlation using *scipy.stats.pearsonr* function on Python v2.7.13 to derive correlation coefficient (r) and *p* value. The correlation is considered significant when *p* is less than 0.05.

3. RESULTS

Full datasets for field measurements and isotope analysis for surface samples are given in the Supplementary Table S1. The measured *Sphagnum* WC varied from 444% to 1928% among all surface *Sphagnum* samples. The maximum WTD was 65 cm at hummock-to-tool transect at site VC. The sites AP and CC had WTD of 42 cm and 70 cm, respectively. Surface *Sphagnum* cellulose $\delta^{13}C$ values ranged from −32.1‰ to −24.1‰, and $\delta^{18}O$ values ranged from 18.0‰ to 21.9‰. The concentrations of *n*-alkanes in surface *Sphagnum* samples ranged from 61 to 152 μg/g dry wt., and their distribution was dominated by *n*-C_{23}, followed by *n*-C_{21} and *n*-C_{25}, confirming *n*-C_{23} as the major biomarker for *Sphagnum* (Fig. S1; Nichols et al., 2006). We observed that *n*-alkane distribution changed with WC (Fig. S2), but we only presented and discussed isotope data in *Sphagnum* leaf wax biomarker *n*-C_{23} hereafter. Surface *Sphagnum* *n*-C_{23} $\delta^{13}C$ values ranged from −42.3‰ to −37.9‰, and *n*-C_{23} δ^2H values ranged from −219.4‰ to −196.4‰. Squeezed *Sphagnum* leaf water δ^2H and $\delta^{18}O$ values ranged from −72.3‰ to −19.1‰, and from −8.9‰ to 0‰, respectively. Bog water δ^2H and $\delta^{18}O$ values ranged from −89.2‰ to −77.1‰, and from −12.1‰ to −10.3‰, respectively, which were distinctly lower than squeezed leaf water data.

Isotope data for long strand samples are given in the Supplementary Table S2. Cellulose $\delta^{13}C$ and $\delta^{18}O$ values along the long strands at site CC (1-cm increments) ranged from −29.5‰ to −28.3‰, and from 18.8‰ to 21.0‰, respectively. These ranges of isotopic variability are smaller for $\delta^{13}C$ and larger for $\delta^{18}O$ than that in surface *Sphagnum* samples at the same site. The concentrations of *n*-alkanes along the CC strands (seven samples) ranged from 51 to 90 μg/g dry wt., and their *n*-C_{23} $\delta^{13}C$ and δ^2H values ranged from −41.7‰ to −40.2‰, and from −216.7‰ to −212.3‰, respectively. Cellulose $\delta^{18}O$ and $\delta^{13}C$ values along the long strands at site VC (2-cm increments) ranged from −29.7‰ to −28.6‰, and from 20.4‰ to 21.4‰, respectively. However, for VC strands, both these ranges of variability are smaller than that in VC surface *Sphagnum* samples, and such narrow variability impeded detecting sub-annual signals on the strands, likely due to the coarser analytical resolution (2 cm increments rather than 1 cm; Fig. S3). We thus only discussed the results from long strands of site CC hereafter.

3.1. Surface *Sphagnum* cellulose isotopic variability across moisture gradient

The overall correlation between cellulose $\delta^{13}C$ and WC among all samples across multiple sites is positive and significant ($r = 0.78$, $p < 0.001$), with lower $\delta^{13}C$ values correlated with drier conditions (Fig. 4a). In contrast, the overall correlation between cellulose $\delta^{18}O$ and WC is negative but not statistically significant at the 95% level ($r = -0.29$, $p = 0.051$). Despite this, their correlations are statistically significant at the regional scale (see caption of Fig. 1) in Karukinka Park ($r = -0.52$, $p < 0.05$) and Laguna Blanca ($r = -0.71$, $p < 0.05$), with higher $\delta^{18}O$ values correlated with drier conditions (Fig. 4b; Table S3).

For the hummock-to-pool transect at site VC, measured WC of *Sphagnum* was closely linked to the available WTD data, capturing localized moisture availability along the microtopographical transect. Towards the drier end of the transect (0–200 cm from hummock top), the range of WC was narrow with a mean of 840% (Fig. 5c). Cellulose samples close to the hummock top had relatively lower $\delta^{13}C$ values (lower than −29.5‰) and high $\delta^{18}O$ values (higher than 19.8‰). The central portion of the transect (200–400 cm from hummock top) was characterized by a clear trend towards higher WC and shallower WTD, with increasing cellulose $\delta^{13}C$ and decreasing cellulose $\delta^{18}O$. The highest $\delta^{13}C$ value (−24.1‰) and the lowest $\delta^{18}O$ value (18.0‰) were recorded from *S. cuspidatum* samples growing at the wettest end of the sampling transect (Fig. 5a and b). Statistically, cellulose $\delta^{13}C$ and $\delta^{18}O$ from site VC showed

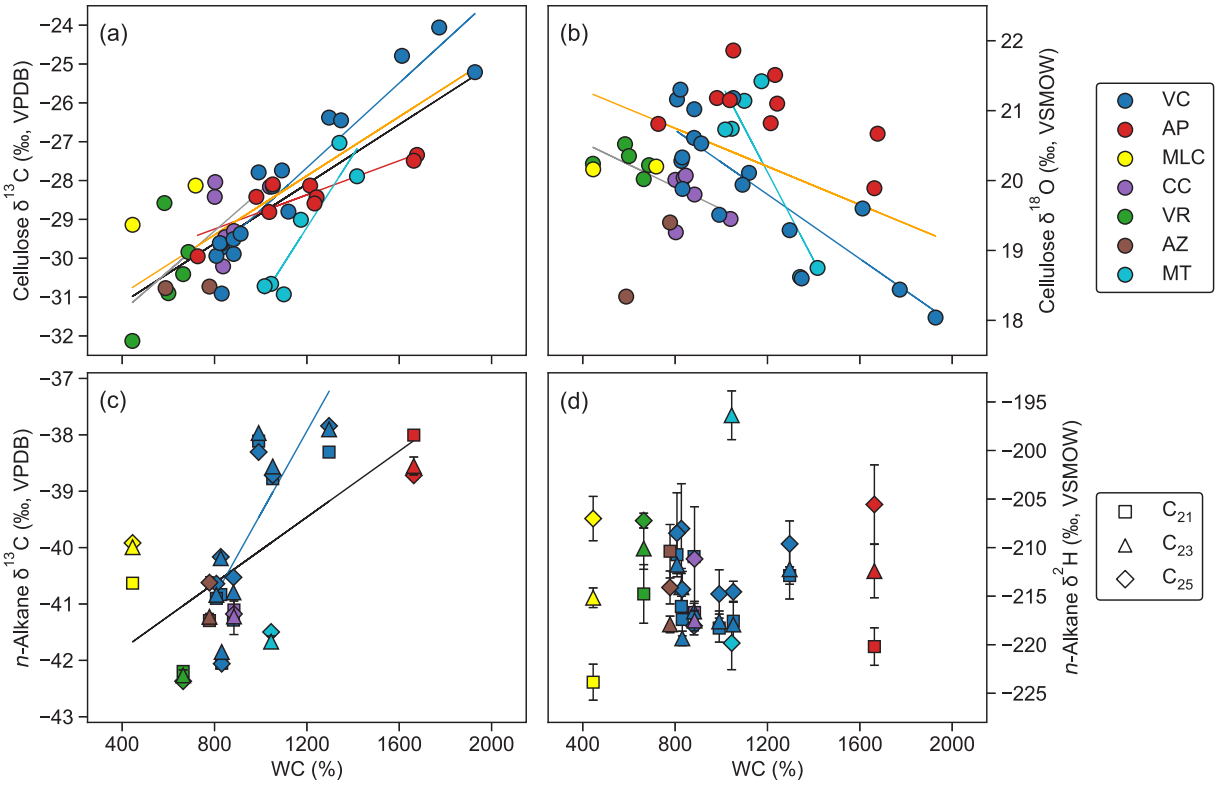

Fig. 4. Scatter plots showing the relationships between (a) *Sphagnum* cellulose $\delta^{13}C$ and water content (WC); (b) cellulose $\delta^{18}O$ and WC; (c) S*phagnum* *n*-alkane $\delta^{13}C$ and WC; and (d) *n*-alkane $\delta^{2}H$ and WC. Scatter colors represent different sites. Error bars in (c) and (d) are standard deviation (1σ) of replicate measurements in compound-specific isotope analysis. Black regression lines indicate significant correlations from all data points. Gray and orange regression lines indicate significant correlations from data points of Laguna Blanca region and Karukinka Park region, respectively. Other colored regression lines indicate site-specific significant correlations. (For interpretation of the references to color in this figure legend, the reader is referred to the web version of this article.)

significant positive and negative correlations with WC, respectively ($r = 0.94$, $p < 0.001$; $r = -0.83$, $p < 0.001$; Fig. 4a and b), even if *S. cuspidatum* data were excluded ($r = 0.92$, $p < 0.001$; $r = -0.72$, $p < 0.01$; Table S3).

At site AP where samples were collected evenly from the edge to the center of peatland along a narrower range of WC than at VC, a significantly positive correlation between cellulose $\delta^{13}C$ and WC was still found ($r = 0.89$, $p < 0.01$; Fig. 4a), but not between cellulose $\delta^{18}O$ and WC ($r = -0.55$, $p = 0.13$; Fig. 4b). At site MT where samples were collected along a mountain slope, the reported significant correlations between cellulose $\delta^{13}C$ and WC ($r = 0.92$, $p < 0.01$) and between cellulose $\delta^{18}O$ and WC ($r = -0.84$, $p < 0.05$) appeared to be driven by two samples (Fig. 4a and b) collected at high elevations, near the alpine treeline (Fig. 2h). However, the site-specific correlations between cellulose $\delta^{13}C$ and WC and between cellulose $\delta^{18}O$ and WC are statistically insignificant at sites VR ($r = 0.58$, $p = 0.31$; $r = -0.29$, $p = 0.64$) and CC ($r = 0.22$, $p = 0.67$; $r = -0.34$, $p = 0.51$), where the ranges of WC were narrow. Despite this, both VR and CC sites are in the same region (Laguna Blanca; Fig. 1), and a statistically significant correlations were achieved if data from both sites were combined ($r = 0.68$, $p < 0.05$; $r = -0.71$, $p < 0.05$; Fig. 4a and b).

3.2. Surface *Sphagnum* leaf wax isotopic variability across moisture gradient

The positive correlation between *n*-C_{23} $\delta^{13}C$ and WC is weaker than cellulose dataset, but still significant ($r = 0.24$, $p < 0.05$; Fig. 4c). We found that the *n*-C_{23} $\delta^{13}C$ data *per se* are highly correlated with their corresponding cellulose $\delta^{13}C$ ($r = 0.93$, $p < 0.001$; Fig. S4), thus the weaker correlation between *n*-C_{23} $\delta^{13}C$ and WC is likely an artifact of selective measurements in *n*-alkane isotope dataset. However, there was no significant correlation between *n*-C_{23} $\delta^{2}H$ and WC ($r = 0.18$, $p = 0.56$; Fig. 4d). Data from seven samples from VC hummock-to-pool transect showed similar pattern (Fig. 5).

3.3. Isotopic relationship among bog water, squeezed leaf water, plant cellulose and leaf wax

Bog water isotope data were plotted very close to either global meteoric water line (GMWL) or local meteoric water lines (LMWL) and were similar to the isotopic composition of mean annual precipitation recorded in Global Network of Isotopes in Precipitation (GNIP; accessed from https://nucleus.iaea.org/wiser) station in Punta Arenas (Fig. 6a).

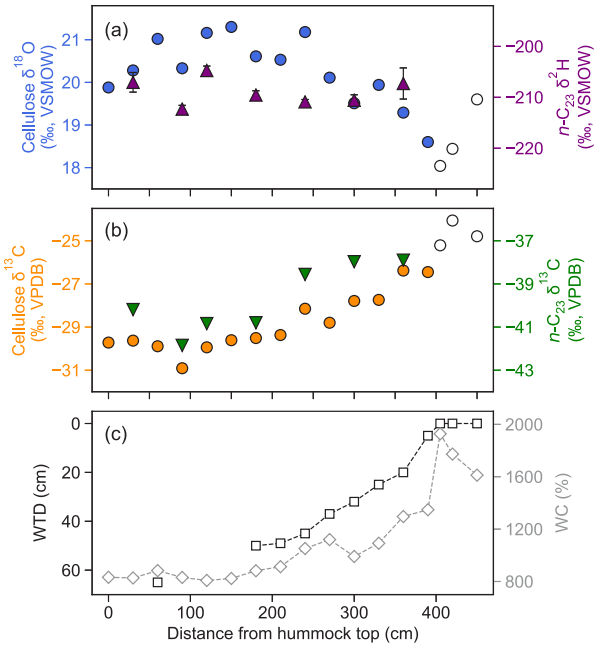

Fig. 5. Variations in *Sphagnum* cellulose and *n*-alkane isotopic compositions along moisture gradient in hummock-to-pool transect at site VC. (a) Cellulose $\delta^{18}O$ (blue circles) and *n*-C_{23} $\delta^{2}H$ (purple triangles). (b) Cellulose $\delta^{13}C$ (orange circles) and *n*-C_{23} $\delta^{13}C$ (green inverted triangles). (c) Measured water table depth (WTD; black squares) at sampling points and measured *Sphagnum* water content (WC; gray diamonds). Open circle symbols in (a) and (b) are data points corresponding to special species *S. cuspidatum*. Error bars in (a) are standard deviation (1σ) of replicate measurements in compound-specific isotope analysis. (For interpretation of the references to color in this figure legend, the reader is referred to the web version of this article.)

Squeezed *Sphagnum* leaf water was more enriched in ^{2}H and ^{18}O, and these leaf water isotope data fell on local *Sphagnum* evaporation lines (referred as LSEL hereafter) at a slope of 4.83, 5.60, and 3.87 in Karukinka Park region, Laguna Blanca region, and site MT, respectively (Fig. 6a). We found that squeezed leaf water $\delta^{18}O$ data were much more scattered than cellulose $\delta^{18}O$ data and they were unexpectedly negatively correlated ($r = -0.48$, $p < 0.01$; Fig. 6b). Interestingly, the higher squeezed leaf water $\delta^{2}H$ and $\delta^{18}O$ values seemed to be associated with the higher WC (Fig. 6b). There was no significant correlation between *n*-C_{23} $\delta^{2}H$, which were selectively analyzed unlike cellulose dataset, and squeezed leaf water $\delta^{2}H$ ($r = 0.28$, $p = 0.35$; Fig. S5).

3.4. Isotopic variability along *Sphagnum* long strands

For *Sphagnum* strands at site CC, stem bifurcations occurred mainly at 7–9 cm and 12–16 cm from capitula (Fig. 7d). Plotting strand cellulose $\delta^{18}O$ data versus each 1-cm strand increment showed a sine function-like pattern, which aligned well with the growing season (likely October–April when average air temperature is higher than 5 °C without snow ground; Daley et al., 2012) monthly precipitation $\delta^{18}O$ data in recent two years (2015 and 2014) recorded by the closest (~130 km away) GNIP station in Punta Arenas (Fig. 7a and b). The *n*-C_{23} $\delta^{2}H$ signals along *Sphagnum* strands showed similar seasonal shifts, but the amplitude of variability was only 4.4‰ (Fig. 7b). A plot of cellulose $\delta^{13}C$ versus stem increment did not show any clear seasonal pattern (Fig. 7c). Noteworthy were the highest $\delta^{13}C$ values in sections of 18–20 cm and the decline in $\delta^{13}C$ towards recent growth, leading to a roughly parallel trend between cellulose $\delta^{13}C$ and Punta Arenas monthly precipitation anomaly record based on the Global Historical Climatology Network (GHCN; accessed from https://www.ncdc.noaa.gov/ghcnm/) data (Fig. 7a and c). The *n*-C_{23} $\delta^{13}C$ data showed a similar decreasing trend as cellulose $\delta^{13}C$ towards recent growth, but with a larger amplitude of shift from −40.1‰ to −41.7‰ (Fig. 7c).

4. DISCUSSION

4.1. Water content (WC) as an indicator of *Sphagnum* moisture availability

To validate the response of paleohydrological proxy to moisture gradient in peatlands, usually WTD rather than plant tissue water content is measured, assuming that a deeper WTD is associated with drier habitat, and vice versa (Markel et al., 2010; Loader et al., 2016; Granath et al., 2018). Indeed, WTD is one of the most important predictors of vegetation distribution and growth in peatlands (Rydin and Jeglum, 2013). In this study, however, we used WC to characterize *Sphagnum* moisture availability at their localized habitats (Van Bellen et al., 2014; Bramley-Alves et al., 2015; Royles et al., 2016), and we argue that WC is an equivalent or even more sensitive moisture indicator than WTD for the following reasons.

First, the difference in the mean and range of WC values between different sites conform to our field observation and sampling strategy (Fig. 4; Table S1). For example, the site VR had a very low mean WC (595%) with a narrow range (243%), and our field observation indicated that this site was a very dry bog and maintained only a weak moisture gradient even across the sampled hummock-to-hollow transect (Fig. 2c). In contrast, the sites VC and AP had high mean WC of 1118% and 1203% with wide ranges of 1120% and 950%, respectively, in agreement with our field observation that these two sites were generally wet (Fig. 2b and e) and with our sampling strategy that maximized the site-specific moisture gradient. WC was not correlated with mean annual precipitation inferred from regional climate model output (Table 1; Fig. S6), suggesting that WC mainly reflects peatland-specific moisture conditions. Second, southern Patagonian peat bogs are usually characterized by WTD as deep as 70 cm (Table S1). As a result, *Sphagnum* capitula on the peatland surface might have weak hydrological connections with the deep peatland water table, while *Sphagnum* mosses typically only access water stored in the top 20 cm of peat (Nichols et al., 2010). The WTD and WC measurements across hummock-to-pool transect at site VC showed congruent trends, but they were not the same: *Sphagnum* samples collected at 60 cm and 180 cm away from hummock top had

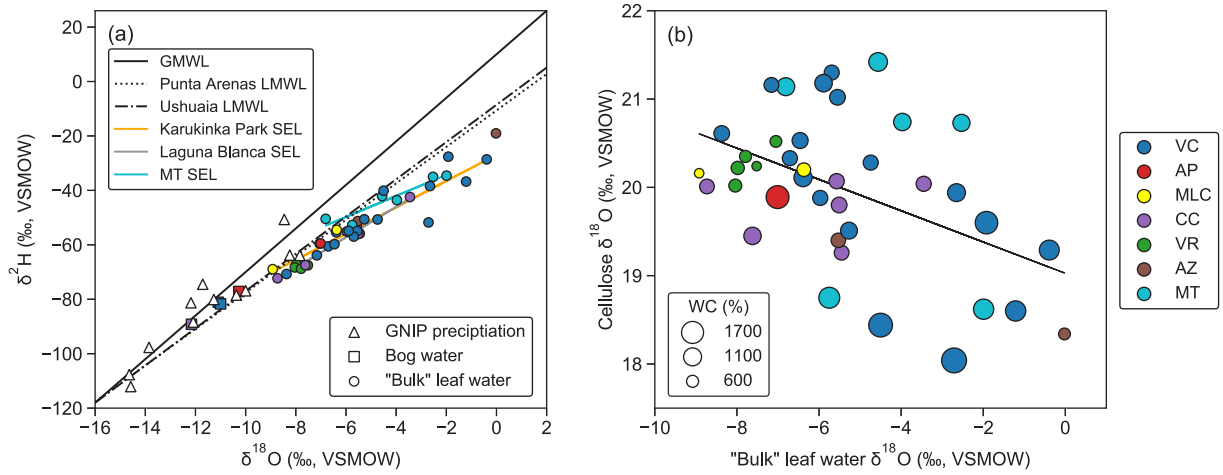

Fig. 6. (a) Scatter plot showing the relationship between δ^2H and $\delta^{18}O$ for monthly precipitation (during year 2015, the year right prior to our sampling excursion in January 2016) based on GNIP data from Punta Arenas (white triangles), bog water (colored squares), and leaf water (colored circles). Global meteoric water line (GMWL; solid black line) and local meteoric water lines (LMWL) derived from Punta Arenas ($\delta^2H = 6.69\ \delta^{18}O–10.65$; during 1990–2015; solid dotted line) and Ushuaia ($\delta^2H = 6.84\ \delta^{18}O – 8.57$; during 1981–2002; solid dash-dotted line) GNIP data are also shown. A few GNIP isotope data that were erroneously positive or were suspected being affected by evaporation were not included to derive LMWLs. Local *Sphagnum* evaporation lines (LSEL) are regressed from leaf water data points of Karukinka Park region ($\delta^2H = 4.83\ \delta^{18}O – 26.90$; orange line), Laguna Blanca region ($\delta^2H = 5.60\ \delta^{18}O – 23.68$; gray line), and site MT ($\delta^2H = 3.87\ \delta^{18}O – 26.60$; cyan line). (b) Scatter plot showing the relationship between cellulose $\delta^{18}O$ and leaf water $\delta^{18}O$. Larger symbols indicate wetter conditions measured by WC. The black regression line indicates significant correlation from all data points. In both (a) and (b), scatter colors represent different sites. (For interpretation of the references to color in this figure legend, the reader is referred to the web version of this article.)

WTD of 65 cm and 50 cm, respectively, but almost identical WC of ~880% (Fig. 5c). Van Bellen et al. (2014) also found that WC was not sensitive to WTD variations if WTD was greater than 40 cm in southern Patagonian peat bogs. Third, WC measurements have been applied to study how photosynthesis and respiration of bryophytes (in particular *Sphagnum*) respond to moisture regimes under controlled laboratory conditions or in the field known as plant–water relations (Dilks and Proctor, 1979; Titus et al., 1983; Rydin and McDonald, 1985; Murray et al., 1989; Rice and Giles, 1996; Schipperges and Rydin, 1998; Royles et al., 2013a). For example, *Sphagnum* mosses have been shown to have the maximum rate of photosynthesis at WC of 700–1000%, while progressively wetter-than-optimum WC would only gently decrease photosynthesis rate but slightly lower-than-optimum WC would drastically slow or even cease photosynthesis (Schipperges and Rydin, 1998). However, field WC measurements were never applied to validate stable isotope proxies in peatlands, and it impeded our understanding how the expression of stable isotope variations in *Sphagnum* was tied to plant physiology.

We acknowledge that our WC measurements represented only "snapshot" moisture conditions that were often complicated by factors including recent rainfall events, morning dew, evapotranspiration, and shading from co-existing vascular plants (Silvola and Aaltonen, 1984; Titus and Wagner, 1984; Murray et al., 1989; Williams and Flanagan, 1996; Van Bellen et al., 2014). Weather station data from Punta Arenas (not shown) indicated that there was only 1.1 mm precipitation at least two weeks prior to sample collection, thus the impact of recent precipitation was very limited. Microtopography is the major driver of WC variability at the time of sample collection as shown in the transect at site VC (Figs. 2b and 5). Therefore, we think that the measured WC represents the moisture gradient in which *Sphagnum* would experience over the majority course of growing season, at least in the one to three months before sample collection. However, it is unclear how the absolute values of WC at each sampling location would change temporally, particularly for hollow microforms where desiccation often occurs (Rydin and Jeglum, 2013). Future studies should collect field *Sphagnum* WC data over the complete growing season to understand its natural short-term and long-term variability at different microforms in peatlands. A few existing studies have shown that the WC of *Sphagnum* displays a degree of stability on daily and monthly scales (Silvola and Aaltonen, 1984; Titus and Wagner, 1984).

4.2. Carbon isotope signatures in *Sphagnum* controlled by the water film effect

Sphagnum mosses growing at different peatland sites are using the same atmospheric CO_2 source for photosynthesis. If recycled CO_2 was insignificant, their cellulose $\delta^{13}C$ should be primarily affected by plant-specific growth conditions. Species effects of leaf anatomy/physiology were excluded in our study as we focused on single species *S. magellanicum*. The significantly positive correlations between cellulose $\delta^{13}C$ and WC, either from a single site or from all sites together, indicate strong sensitivity of *Sphagnum* cellulose $\delta^{13}C$ to moisture availability, as explained by the water film effect (Fig. 4a). A few additional measurements on wet-adapted species *S. cuspidatum*—

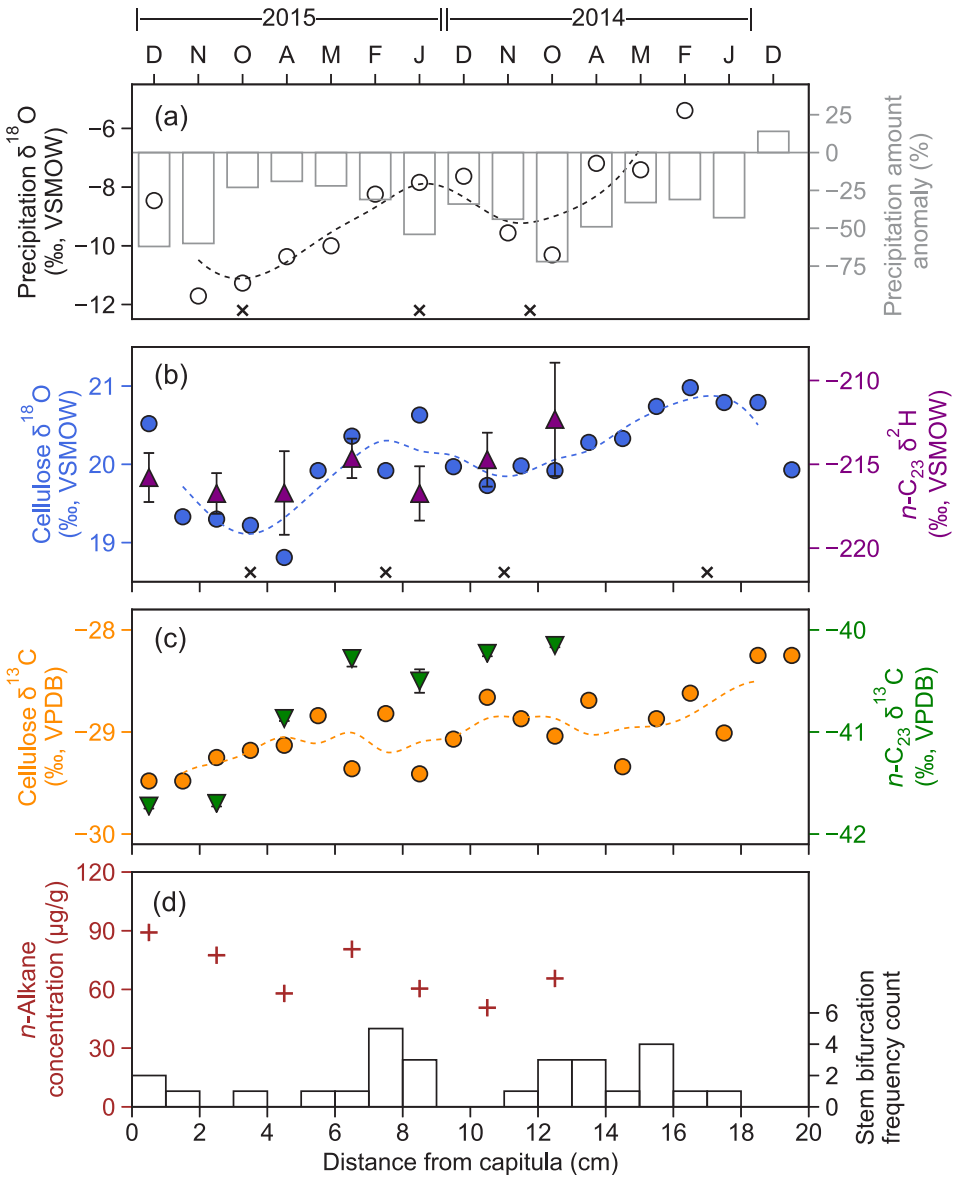

Fig. 7. Changes in *Sphagnum* cellulose and *n*-alkane isotopic compositions along *Sphagnum* strands at site CC. (a) Growing season monthly precipitation $\delta^{18}O$ values (open circles with three-point average dashed spline line) based on GNIP data from Punta Arenas. The top *x*-axis is time (month), with tick labels D, N, O, A, M, F, and J, refer to December, November, October, April, March, February, and January, respectively. Other months are not considered within the growing seasons. The $\delta^{18}O$ values for January 2014 and December 2013 were erroneously positive and were not shown. The bar chart plotted on the right *y*-axis is Punta Arenas monthly percentage of precipitation anomaly relative to its long-term monthly mean, based on data from the Global Historical Climatology Network (GHCN). (b) *Sphagnum* strand cellulose $\delta^{18}O$ (blue circles with three-point average spline line) and *n*-C_{23} $\delta^{2}H$ (purple triangles) versus distance from *Sphagnum* capitula. The cross symbols at bottom of (a) and (b) marked the local minimum and maximum $\delta^{18}O$ in three-point average spline lines, which were used as tie points to determine stem incremental rate. (c) *Sphagnum* strand cellulose $\delta^{13}C$ (orange circles with three-point average spline line) and *n*-C_{23} $\delta^{13}C$ (green inverted triangles) from the same sample with (b). (d) *n*-Alkane concentrations in analyzed leaf wax samples. Histogram at bottom is the frequency count of stem bifurcation positions on *Sphagnum* strands. (For interpretation of the references to color in this figure legend, the reader is referred to the web version of this article.)

which possesses triangle-shaped photosynthetic cells exposed at the leaf surface instead of being enclosed by hyaline cells as in *S. magellanicum* (Rice and Giles, 1996; Loisel et al., 2009)—showed very high cellulose $\delta^{13}C$ values (−24.7‰ on average) that characterized strong CO_2 diffusional resistance at extreme wetness, consistent with WC data (Fig. 5b). It suggested that any species effects of leaf anatomy were overprinted by the expression of water film effect. Furthermore, a previous study showed that the pool species *S. cuspidatum* could have $\delta^{13}C$ value as low as −34.7‰ (Proctor et al., 1992), which indicated the contribution of recycled CO_2 in wet habitat, but in our dataset, there was no sign of extremely negative $\delta^{13}C$ signals caused by recycled CO_2. However, we also found that cellulose

$\delta^{13}C$ and mean annual precipitation inferred from regional climate output had a weak, but significant, cross-site negative correlation ($r = -0.32$, $p < 0.05$), in opposite to the water film effect (Fig. S6). Although the mechanism for this observation was unclear, hereafter we only discuss the WC effect that exhibited strong and multi-level control on cellulose $\delta^{13}C$.

Sphagnum n-C_{23} $\delta^{13}C$ data also support the water film effect (Fig. 4c), and the strong correlation between n-C_{23} $\delta^{13}C$ and cellulose $\delta^{13}C$ with a regression equation slope of 1.01 (Fig. S4) implied that moisture gradient affected cellulose and n-alkanes $\delta^{13}C$ similarly. The interception in regression function perhaps mean the offset of fractionation (~10.7‰) between n-alkane and cellulose biosynthesis (Fig. S4).

4.3. Cellulose oxygen isotope signatures in *Sphagnum* influenced by evaporative enrichment

It has been well understood that *Sphagnum* cellulose $\delta^{18}O$ is controlled by source water $\delta^{18}O$ by an offset of biochemical enrichment factor, but source water in *Sphagnum* leaves likely has been additionally modified by evaporative enrichment relative to precipitation input (Price et al., 2009; Loader et al., 2016). If precipitation $\delta^{18}O$ was invariant and if the degree of evaporative enrichment of ^{18}O in leaf water was higher in drier *Sphagnum* (Ménot-Combes et al., 2002), we would expect a negative correlation between cellulose $\delta^{18}O$ and WC. Our data showed such negative correlations at site-specific scale and at regional scale (Fig. 4b), supporting the strong influence of evaporative enrichment on *Sphagnum* cellulose $\delta^{18}O$ signals. However, correlation was insignificant when data from all sites were combined. This could be explained by certain spatial variability in precipitation $\delta^{18}O$ signals induced by local topography and air-mass trajectories in terrain-complex Patagonia (Daley et al., 2012; Xia et al., 2018). Despite a lack of regional precipitation isotope measurements, our opportunistic samples of bog water that isotopically were close to yearly averaged precipitation indicated that precipitation $\delta^{18}O$ in Laguna Blanca region might be 1–2‰ lower than in Karukinka Park region (Fig. 6a).

However, our squeezed leaf water isotope data appeared to not support the idea that evaporative enrichment of ^{18}O was progressively larger with lower WC. Although our sampling approach can only collect ephemeral "bulk" leaf water during that particular day rather than over a time span, the significantly negative relationship between cellulose and squeezed leaf water $\delta^{18}O$ ($r = -0.48$, $p < 0.01$; Fig. 6b) is contradictory to the physiological models that have been widely tested. This observation is similar to another study on New Zealand peatland rushes (*Empodisma* spp.) that found root cellulose $\delta^{18}O$ was negatively correlated with root water and precipitation $\delta^{18}O$ (Amesbury et al., 2015). We also suggested that this observation in *Sphagnum* may provide some insights into the nature of metabolic water in *Sphagnum* leaves.

The most plausible explanation is that our "bulk" leaf water collected by squeezing the capitula did not represent the metabolic water used for cellulose biosynthesis. *Sphagnum* have great water retention capacity by hyaline cells in the leaves and the outer cortex of the stems, but most of the water is stored between the leaves known as external capillary spaces, i.e., outside hyaline cells (Murray et al., 1989; Rydin and Jeglum, 2013). This external capillary water is an essential functional component in the physiology of many bryophytes (Dilks and Proctor, 1979; Proctor et al., 1998). Fig. 6b showed that *Sphagnum* with higher WC tended to have higher squeezed leaf water $\delta^{18}O$, and statistical analysis suggested they were positively correlated ($r = 0.46$, $p < 0.01$). If *Sphagnum* with higher WC had higher percentage of water outside hyaline cells and if this fraction of external water was strongly modified by unsteady-state evaporation, our squeezed leaf water would be biased towards higher $\delta^{18}O$ values that might not represent the isotopic composition of leaf water inside hyaline cells (internal water), driving the observed negative correlation. This situation is very likely, as the laboratory experiment by Price et al. (2009) found that their squeezed "pore water" in the top 5 cm section of *Sphagnum* peat had the $\delta^{18}O$ value over 6‰ higher than irrigated water after just one day. Another recent study also proposed that *Sphagnum* capitula water collected by squeezing had been more evaporatively enriched relative to the net isotopic composition of the water (here we called "internal water") used for cellulose biosynthesis (Loader et al., 2016), supporting our speculation.

Furthermore, drier *Sphagnum* such as those growing on hummocks could allocate resources into structural carbohydrates at the cost of metabolic carbohydrates and this strategy aided in maintaining high water retention capacity (Turetsky et al., 2008). As a result, *Sphagnum* in drier habitat could survive dry conditions and still grow, and their cellulose $\delta^{18}O$ might be able to record a moderate degree of evaporative enrichment signal (Aravena and Warner, 1992). In contrast, wetter *Sphagnum* such as those growing in hollows or pools had higher collective surface area and could dry out quickly, thus their growth was limited by desiccation (Rydin and Jeglum, 2013). As a result, *Sphagnum* in depressions might cease to grow and fail to register evaporative enrichment signal. However, our field observation found no sign of desiccation for *Sphagnum* growing in depressions during sampling, such as the pool in the site VC (Fig. 2b). In fact, at this site *S. cuspidatum* floating on the edge of pool had the lowest cellulose $\delta^{18}O$ value (18.0‰; Fig. 5b), while pool water likely was highly enriched in ^{18}O due to exposure to air. Instead, we further speculate that for *Sphagnum* with higher WC their internal water was partitioned and protected from evaporation by the presence of thicker external water, thus their metabolic water likely was rarely modified by evaporative enrichment, but isotope signals of this internal water were poorly represented in that of squeezed leaf water we measured.

The median enrichment factor between squeezed leaf water and cellulose $\delta^{18}O$ was 26.0‰, but if we used precipitation $\delta^{18}O$ in the recent one to three months from Punta Arenas GNIP data as the source water input, the median enrichment factors would range from 28.5‰ to 30.7‰ (Fig. S7). Although the uncertainty in biochemical fraction-

ation of cellulose biosynthesis has been estimated as ±1‰ (Daley et al., 2010) or ±3‰ (Zanazzi and Mora, 2005), the widely accepted value of 27‰ (Sternberg, 2009) was above the enrichment factor calculated from squeezed leaf water data, but below the enrichment factor calculated from precipitation data, suggesting that internal metabolic leaf water were indeed enriched in ^{18}O relative to precipitation, but not as much as our measured values from squeezed leaf water suggested.

4.4. Leaf wax hydrogen isotopes in *Sphagnum* insensitive to moisture gradient

Although *Sphagnum* cellulose $\delta^{18}O$ data showed sensitivity to record evaporative enrichment of ^{18}O in metabolic leaf water, the *n*-C_{23} $\delta^{2}H$ signals showed a muted response to moisture gradient and did not record the evaporative enrichment of ^{2}H in proportional to that was expressed in cellulose $\delta^{18}O$ dataset (Figs. 4d and 5a). This requires explanation, and we propose two possible mechanisms below.

First, in general biochemical fractionations in hydrogen isotopes are much more complex than in oxygen isotopes (Yakir, 1992; Sachse et al., 2012). The pathway of biochemical fractionation in cellulose $\delta^{18}O$ lies in the post-photosynthetic (heterotrophic) exchange reactions during carbonyl hydration, with a well-conservative enrichment factor centered at ~27‰ for cellulose relative to source water (Sternberg et al., 1986; Sternberg, 2009). However, biochemical fractionations of hydrogen isotopes in either cellulose or *n*-alkanes represent a balance between autotrophic and heterotrophic metabolisms that resulted in ^{2}H depletions and enrichments in carbohydrate intermediates, respectively (Yakir, 1992; Sessions et al., 1999). A series of hydrogen addition, removal, and isotopic exchange reactions are involved in heterotrophic processing of carbohydrates (Sachse et al., 2012; Mora and Zanazzi, 2017). As a result, the hydrogen atoms on the final *n*-alkane products could originate from metabolic leaf water, biosynthetic precursors, and NADPH (Sessions et al., 1999; Sachse et al., 2012). *Sphagnum* metabolic leaf water $\delta^{2}H$ variations, if any, might be smoothed in *n*-alkane $\delta^{2}H$ due to complex hydrogen isotope fractionation pathway.

Second, kinetic fractionation of hydrogen isotopes is smaller than oxygen isotopes. Evaporation of leaf water involves both equilibrium and kinetic isotope effects. The equilibrium fractionation factor for hydrogen isotopes differs from oxygen isotopes by a well-known factor of ~8, which accounts for the slope of GMWL in $\delta^{2}H$–$\delta^{18}O$ space. A lower kinetic fractionation factor for hydrogen isotopes than oxygen isotopes accounts for the lower slope of local evaporation line (LEL) than GMWL, the former of which typically is in the range from 5 to 7. That said, theoretical prediction of the LEL (Mayr et al., 2007) is based on the Craig–Gordon model (Craig and Gordon, 1965). Again, *Sphagnum* mosses lack stomata and evaporate leaf water through tiny pores on hyaline cells, preventing liquid-vapor interaction. Therefore, the Rayleigh model better characterizes the evaporation process in *Sphagnum* hyaline cells (Nichols et al., 2010):

$$\ln f = -\frac{\delta_s - \delta_p}{\varepsilon_e + \varepsilon_k} \tag{3}$$

where δ_s and δ_p are the isotopic composition of *Sphagnum* leaf water and precipitation, respectively; ε_e and ε_k are the equilibrium and kinetic enrichment factors, respectively; and f is the fraction of water remaining after evaporation. Then the slope (S) of LSEL under gradual *Sphagnum* leaf water loss is:

$$S = \frac{\varepsilon_e^H + \varepsilon_k^H}{\varepsilon_e^O + \varepsilon_k^O} \tag{4}$$

where ε_e^H and ε_k^H are the equilibrium and kinetic enrichment factors for hydrogen isotopes, respectively, and ε_e^O and ε_k^O are the equilibrium and kinetic enrichment factors for oxygen isotopes, respectively. As an exercise, we used an average summer mid-day time temperature (17.4 °C or 290.55 K) and relative humidity (70.0%; Loader et al., 2016) representative for southern Patagonian peat bog conditions to derive these enrichment factors based on previously established models (Gonfiantini, 1986; Horita and Wesolowski, 1994): the ε_e^H, ε_k^H, $\varepsilon_e^O$and $\varepsilon_k^O$are 83.83‰, 3.75‰, 9.96‰ and 4.26‰, respectively. Then Eq. (4) predicted a model-based slope of LSEL at 6.15 under an ideal Rayleigh process. If the model accurately described the moss leaf water evaporation, it implied that $\delta^{2}H$ increased by only 6‰ (compared to 8‰) when $\delta^{18}O$ increased by 1‰ in evaporated *Sphagnum* leaf water. This increase in leaf water $\delta^{2}H$ was only 1.9 times as large as the analytical uncertainty (1σ) in *n*-alkane $\delta^{2}H$, but for cellulose $\delta^{18}O$ it was 4.5 times as large.

However, the model-based slope of LSEL was lower than the slopes regressed empirically from squeezed leaf water isotope data, the latter of which from our dataset were as low as 3.87, 4.83, and 5.60 (Fig. 6a), and from Loader et al. (2016) were 3.01 and 6.03. Again, these squeezed leaf water samples might not represent internal metabolic leaf water, but they had been mixed with external water between leaves. The lower slopes observed than modelled might indicate the importance of atmospheric water vapor exchange with external leaf water, which could affect the slopes of evaporation lines (Mayr et al., 2007). Therefore, reliable approaches to collect plant tissue water in waterlogged peatlands must be further explored to test the hypothesis on the separation of internal and external leaf water and to study peatland isotope hydrology and plant physiology (Amesbury et al., 2015).

4.5. Relationships between cellulose carbon and oxygen isotopes

As both *Sphagnum* cellulose $\delta^{13}C$ and $\delta^{18}O$ exhibited sensitivity to moisture gradient, scatter plots of cellulose $\delta^{18}O$ vs. $\delta^{13}C$ showed negative correlations (Fig. 8), which were significant at sites VC ($r = -0.80$, $p < 0.001$) and MT ($r = -0.81$, $p < 0.05$), as well as among Karukinka Park region ($r = -0.67$, $p < 0.001$), but not at the other sites (Table S3). The reason for insignificant relationships at other sites might be due to insufficient data points or narrow WC gradients. Our analysis of cellulose isotope data

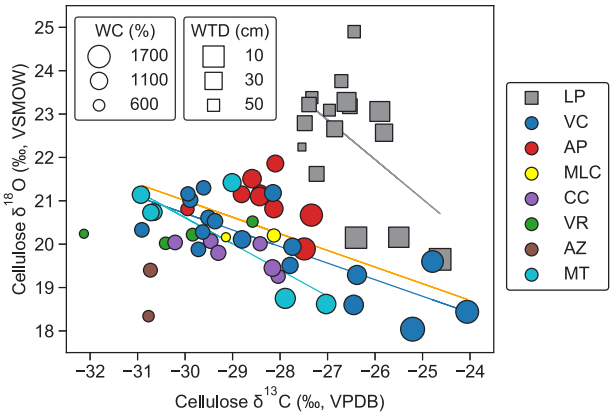

Fig. 8. Scatter plot showing the relationship between *Sphagnum* cellulose $\delta^{13}C$ and $\delta^{18}O$ data from every site in this study, plus data from site LP (Loader et al., 2016). Larger symbols indicate wetter conditions measured by WC (sites from this study) or WTD (site LP where WC was not measured). Scatter colors represent different sites. Site-specific significant correlations are indicated by colored regression lines. Note that cellulose was extracted from *Sphagnum* capitula in Loader et al. (2016), while cellulose was extracted from *Sphagnum* stems in this study. (For interpretation of the references to color in this figure legend, the reader is referred to the web version of this article.)

reported at another study site Laguna Parrillar (LP; Loader et al., 2016) with samples collected across a transect with multiple hummocks and hollows also showed a significantly negative correlation ($r = -0.51$, $p < 0.05$; Fig. 8).

Therefore, we report, for the first time to our knowledge, the intrinsic relationship between two isotope ratios in *Sphagnum*. We show that, in *S. magellanicum*, moisture availability influences cellulose $\delta^{13}C$ via water film effect on discrimination against $^{13}CO_2$ and similarly can imprint on cellulose $\delta^{18}O$ via evaporative enrichment of ^{18}O in metabolic leaf water. Our additional observation on wet-adapted species *S. cuspidatum* showed that their isotope data were in the same trajectory as *S. magellanicum* data at the VC transect (Fig. 5a and b). This finding is in line with increasing evidence that *Sphagnum* species-specific effects on biochemical fractionations are minimal, and that the observed inter-species differences in isotopic composition can largely be explained by their favored ecological ranges rather than by any divergences in isotopic fractionation metabolism (Rice and Giles, 1996; Loisel et al., 2009; Daley et al., 2010; El Bilali and Patterson, 2012).

More empirical data are needed to investigate if the observed relationships are robust among different species and are consistent in different regions. A caveat given by Royles and Griffiths (2015) is that bryophyte cellulose carbon isotope signal reflects the condition of maximum CO_2 assimilation, while oxygen isotope signal mainly reflects the condition of maximum cellulose biosynthesis. This temporal separation in photosynthesis and cellulose biosynthesis has been demonstrated in a controlled laboratory experiment on a desiccation-tolerant moss species *Syntrichia ruralis* (Royles et al., 2013a). This moss species experiences substantial daily fluctuations in WC, attaining moisture rapidly following a rainfall event or early morning dew and then drying out completely in hours. The maximum cellulose biosynthesis occurs at saturation (with a WC of 400%), while the maximum CO_2 assimilation occurs at substantial desiccation (with a WC of 110%) but before complete desiccation (Royles et al., 2013a). It likely also explained a lack of correlation between cellulose $\delta^{13}C$ and $\delta^{18}O$ in Antarctic peatbank mosses *Chorisodontium aciphyllum* and *Polytrichum strictum* from non-waterlogged habitats that do not have a persistent external water film (Royles et al., 2012; Royles and Griffiths, 2015). In contrast, *Sphagnum* mosses inhabit waterlogged peatlands, retain water in their hyaline cells, have a well-developed capillary network, and maintain a persistent external water film. As a result, the short-term variation of WC is relatively much less variable (Silvola and Aaltonen, 1984; Titus and Wagner, 1984) and its influence on physiological function is minimal for this genus. The correlation between *Sphagnum* cellulose $\delta^{13}C$ and $\delta^{18}O$ suggests a possible convergence in the timing of CO_2 assimilation and cellulose biosynthesis. Undertaking experimental studies on *Sphagnum* under controlled laboratory condition is also useful to understand the coupled processes between carbon and water (H and O) isotope fractionations (Brader et al., 2010). More importantly, ecophysiological modeling on the *Sphagnum* water film effect on $\delta^{13}C$ will be useful as it can tie carbon isotope fractionation caused by water resistance of CO_2 diffusion to oxygen isotope fractionation explained by the evaporation model. The coupled water film and evaporation model could predict the theoretical value of slope in cellulose $\delta^{13}C$–$\delta^{18}O$ relationship to be compared with empirical regression values, which from our data ranged from −0.91 to −0.38 (Table S3). However, our two-tailed *t*-test with pooled variance (Armitage et al., 2001) suggested that these empirical slope values were not significantly different from each other (Table S4), thus modeling efforts may offer new insights.

4.6. Isotopic signals in *Sphagnum* strand increments document recent growing season conditions

We acknowledge that the phase matching between strand cellulose $\delta^{18}O$ and GNIP precipitation $\delta^{18}O$ data was arbitrary, and that moss growth was still likely during months with snow ground (May–September). However, the robust correspondence between our cellulose $\delta^{18}O$ "time-series" from long strands at site CC and the GNIP precipitation $\delta^{18}O$ record at Punta Arenas, including the relatively low $\delta^{18}O$ values in 2015 and relatively high $\delta^{18}O$ values in 2014, suggested that stem increments of *Sphagnum* could record monthly and seasonal changes in precipitation $\delta^{18}O$ signal over their growing seasons (Fig. 7a and b). The amplitude of observed GNIP precipitation $\delta^{18}O$ variability (6.3‰ and 4.5‰ for monthly data and three-month averaged data, respectively) was more than twice as large as the variability in cellulose $\delta^{18}O$ data (2.2‰ and 1.7‰ for individual and three-point average data, respectively; Fig. 7a and b). This discrepancy could partly be explained by newly proposed temperature-dependence of biochemical fractionation factor during cellulose biosynthesis that might play a larger role on seasonal scale

(Sternberg and Ellsworth, 2011). In Punta Arenas, mean air temperature during the warmest month is ~5 °C higher than that of shoulder seasons (spring and autumn). Based on the Sternberg and Ellsworth (2011) model, temperature seasonality could account for ~1.6‰ difference in ε_b, which would dampen seasonal variability in cellulose $\delta^{18}O$, although temperature-dependence hypothesis was recently challenged by Zech et al. (2014). Another possibility is about *Sphagnum* metabolic leaf water turnover time, which, if lasting for months, could partly explain the dampened variability in cellulose. The *n*-C_{23} δ^2H signals along *Sphagnum* strands showed similar seasonal shifts, but the amplitude of variability is only 4.4‰ (10.3‰ if 1σ error was considered; Fig. 7b). This might be explained by the same reason for the lack of variability in surface *Sphagnum* *n*-C_{23} δ^2H data or that combining ten individual strand sections for lipid extraction would smooth out much the actual isotopic signals on each individual strand.

The apparent seasonal cycle that was recorded in the *Sphagnum* strands implied rapid strand increment at an average rate as high as 1.13 ± 0.05 cm/month (error was standard deviation, 1σ) estimated by matching the tie points (Fig. 7a and b), although we do not have direct dating evidence on the exact "age" of *Sphagnum* strands. This value is much higher than the average *Sphagnum* growth rates reported from boreal peatlands (Loisel et al., 2012), but consistent with the notion that Patagonian peatlands could have several times higher peat accumulation rates than boreal counterparts due to weak temperature seasonality and an even distribution of precipitation throughout the year (Loisel and Yu, 2013a). In addition, the measured WC at site CC (869% in average) is right within the optimal range of WC (700–1000%), by which *Sphagnum* gain maximum rate of photosynthesis (Schipperges and Rydin, 1998). Notably, *Sphagnum* growth rate in the literature was usually measured by the cranked wire method (Clymo, 1970; Loisel et al., 2012), which may underestimate the strand incremental rate due to disturbance and compaction (Fig. 2a and b). Laboratory controlled experiments by Brader et al. (2010) showed that strand increment rates for *S. magellanicum* were 0.92 ± 0.10 and 0.75 ± 0.12 cm/month (error was standard deviation, 1σ, in their original study) in their specified dry and wet conditions, respectively, which were actually slower than other *Sphagnum* species. A field study in New Zealand showed that the dominant *S. cristatum* could have strand increment rates between 0.75 and 3 cm/month during growing seasons (Stokes et al., 1999). Our rapid *Sphagnum* growth rate inferred from the incremental $\delta^{18}O$ data is also supported by other relevant observations: (1) stem bifurcations that occur frequently in summer and autumn, but not in spring (Sobotka, 1976), have a rhythm at every ~7 cm (Fig. 7d); (2) high concentrations of *n*-alkanes match the summer season during which water deficits occurred (Charman, 2007) and more leaf waxes were produced to prevent water loss (Fig. 7d); and (3) the decline in cellulose and leaf wax $\delta^{13}C$ towards recent growth increments (Fig. 7c), likely responding to drier conditions, is consistent with a large negative precipitation anomaly (60% less precipitation than normal), and the highest cellulose $\delta^{13}C$ values at 18–20 cm section (Fig. 7c) match the only month of positive precipitation anomaly (Fig. 7d).

4.7. Implications for peat-based paleoclimate reconstructions

Our modern process study on *Sphagnum* strands showed that the temporal changes in *Sphagnum* strand cellulose $\delta^{18}O$ track monthly and seasonal changes in precipitation $\delta^{18}O$, but cellulose $\delta^{18}O$ values in surface *Sphagnum* samples along a moisture gradient are primarily influenced by moisture availability and evaporative enrichment. This begs the question about which environmental signal is primarily preserved in peat records over longer timescales. We here propose that paired carbon and water (H or O) isotope measurements in *Sphagnum* cellulose or leaf wax biomarker can be used as a new approach to constrain the effect of moisture availability and associated evaporative enrichment effect, in order to extract precipitation $\delta^{18}O$ signal in peat-based climate reconstructions.

Interpreting peat-based proxy-climate data is often complicated by mixture of autogenic (ecological) and allogenic (climatic) processes that would complicate proxy-climate relationships (Swindles et al., 2012). For example, cyclic alternations between wet- and dry-adapted plant macrofossils in peat records from the same region could have a site-specific frequency, which could be caused by ecohydrological feedback and autogenic processes in vegetation patterning (Loisel and Yu, 2013b). Therefore, multiple peat records from the same region are often needed to identify any regionally consistent signals that could have been caused by climate shifts (Barber et al., 2000; Barber et al., 2003; Booth et al., 2006).

We found that in southern Patagonian peat bogs surface *Sphagnum* cellulose $\delta^{13}C$ and $\delta^{18}O$ are negatively correlated in modern settings as a response to a common moisture gradient. Were *Sphagnum* cellulose $\delta^{13}C$ and $\delta^{18}O$ also negatively correlated in peat-core profiles, this would suggest that moisture availability and evaporative enrichment were the dominant factors controlling cellulose $\delta^{13}C$ and $\delta^{18}O$ variations that were not necessarily driven by climate shifts. For example, in peat records, a concurrent shift to higher $\delta^{13}C$ and lower $\delta^{18}O$ values could be explained by a climate-driven increase in bog surface wetness along with a decrease in precipitation $\delta^{18}O$ as in Roland et al. (2015), but it could alternatively be explained by a non-climate-driven ecohydrological feedback, such as a shift from a dry to wet microform (Loisel and Yu, 2013b) that would decrease evaporative enrichment in ^{18}O. However, if there were a lack of negative correlations, it would indicate that the down-core variations in cellulose $\delta^{18}O$ reflected climate-driven shift in precipitation $\delta^{18}O$. For example, our *Sphagnum* cellulose isotope records from a peat bog in Patagonia showed sustained positive correlations between $\delta^{13}C$ and $\delta^{18}O$ time series: higher cellulose $\delta^{13}C$ intervals implying wetter conditions were associated with higher cellulose $\delta^{18}O$ intervals that could not be explained by enhanced evaporative enrichment in ^{18}O, but rather indicated an increase in precipitation $\delta^{18}O$ (Xia et al., 2018). Therefore, in this case, although variations in cellulose $\delta^{13}C$ could still be non-climate-driven, coupling

cellulose $\delta^{13}C$ and $\delta^{18}O$ as a pair has the potential to deconvolve the precipitation $\delta^{18}O$ signal from local ecohydrological noises due to evaporative enrichment. This "dual isotopes" approach is also suitable for *Sphagnum* leaf wax biomarker analysis in peat, given that many postglacial and Holocene peat deposits tend to contain poorly preserved *Sphagnum* macrofossils. *Sphagnum* n-C_{23} δ^2H data that showed insensitivity to modern moisture gradient could be used to infer large-scale shift in precipitation δ^2H after the fractionation factor between n-C_{23} and source water δ^2H is further constrained (Fig. S7).

The coupling of isotopic fractionations associated with carbon and water cycling should be further explored empirically in *Sphagnum*-dominated peatlands as well as in other peat-forming ecosystems such as peatbanks in the Antarctic Peninsula (Royles and Griffiths, 2015). The correlations between moss carbon and water (H or O) isotope ratios could be further constrained by undertaking experimental studies under controlled laboratory conditions or by quantifying the coupling between water film and evaporation effects using ecophysiological models. Such studies would expand the toolbox in the study of peat-climate dynamics.

5. CONCLUSIONS

Cellulose and n-alkane $\delta^{13}C$ of dominant species *Sphagnum magellanicum* in southern Patagonian peat bogs were sensitive to local moisture gradients measured by water content and were strongly controlled by the water film effect. Cellulose $\delta^{18}O$ also showed a moderate response to local moisture gradient brought by differential evaporative enrichment in ^{18}O in metabolic leaf water, but n-alkane δ^2H showed a muted response, likely because hydrogen isotopes have a more complex biochemical fractionation pathway and a smaller kinetic fractionation during leaf water evaporation. Because both *Sphagnum* cellulose $\delta^{13}C$ and $\delta^{18}O$ showed response to local moisture gradient, they were negatively correlated in modern setting. The coupled *Sphagnum* carbon and water isotope fractionations observed in our study provided a conceptual model to interpret peat-core isotope data for paleoclimate reconstruction and should be further understood by more observational data, laboratory experiments, and ecophysiological modeling. Rapidly growing *Sphagnum* strands in southern Patagonia could document monthly-to-seasonal changes in precipitation $\delta^{18}O$, confirming the sensitivity of *Sphagnum* cellulose to record long-term changes in precipitation $\delta^{18}O$ in peat cores. Even if such signals were complicated by evaporative enrichment or autogenic peatland process, paired cellulose $\delta^{13}C$ and $\delta^{18}O$ measurements will constrain peatland paleohydrology and aid in interpreting cellulose $\delta^{18}O$ time series by examining the down-core correlation between cellulose $\delta^{13}C$ and $\delta^{18}O$ data.

ACKNOWLEDGMENTS

We thank Rodrigo Munzenmayer, Alejandro Kusch and Daniel Terán from Karukinka Park, Chile (Wildlife Conservation Society) for permission and logistical support; Jan Lenaerts from University of Colorado Boulder for sharing high-resolution regional climate model output data; four anonymous reviewers for their constructive comments that substantially improved the manuscript; and Associate Editor Tom Wagner for editorial assistance. The work was supported by the U.S. National Science Foundation grants EAR-1502891 to Z. Yu and EAR-1502455 to Y. Huang.

APPENDIX A. SUPPLEMENTARY MATERIAL

Supplementary data to this article can be found online at https://doi.org/10.1016/j.gca.2020.03.034.

REFERENCES

Amesbury M. J., Charman D. J., Newnham R. M., Loader N. J., Goodrich J., Royles J., Campbell D. I., Keller E. D., Baisden W. T., Roland T. P. and Gallego-Sala A. V. (2015) Can oxygen stable isotopes be used to track precipitation moisture source in vascular plant-dominated peatlands?. *Earth Planet Sci. Lett.* **430** 149–159.

Anderson W. T., Bernasconi S. M., McKenzie J. A., Saurer M. and Schweingruber F. (2002) Model evaluation for reconstructing the oxygen isotopic composition in precipitation from tree ring cellulose over the last century. *Chem. Geol.* **182**, 121–137.

Aravena R. and Warner B. G. (1992) Oxygen-18 composition of *Sphagnum*, and microenvironmental water relations. *Bryologist* **95**, 445–448.

Armitage P., Berry G. and Matthews J. N. S. (2001) *Statistical Methods in Medical Research*, fourth ed. Wiley-Blackwell, Malden, MA, USA.

Barber K. E., Maddy D., Rose N., Stevenson A. C., Stoneman R. and Thompson R. (2000) Replicated proxy-climate signals over the last 2000 yr from two distant UK peat bogs: new evidence for regional palaeoclimate teleconnections. *Quat. Sci. Rev.* **19**, 481–487.

Barber K. E., Chambers F. M. and Maddy D. (2003) Holocene palaeoclimates from peat stratigraphy: macrofossil proxy climate records from three oceanic raised bogs in England and Ireland. *Quat. Sci. Rev.* **22**, 521–539.

Bilali H. E., Patterson R. T. and Prokoph A. (2013) A Holocene paleoclimate reconstruction for eastern Canada based on $\delta^{18}O$ cellulose of *Sphagnum* mosses from Mer Bleue Bog. *Holocene* **23**, 1260–1271.

Booth R. K., Notaro M., Jackson S. T. and Kutzbach J. E. (2006) Widespread drought episodes in the western Great Lakes region during the past 2000 years: Geographic extent and potential mechanisms. *Earth Planet. Sci. Lett.* **242**, 415–427.

Brader A. V., van Winden J. F., Bohncke S. J. P., Beets C. J., Reichart G.-J. and de Leeuw J. W. (2010) Fractionation of hydrogen, oxygen and carbon isotopes in n-alkanes and cellulose of three *Sphagnum* species. *Org. Geochem.* **41**, 1277–1284.

Bramley-Alves J., Wanek W., French K. and Robinson S. A. (2015) Moss $\delta^{13}C$: an accurate proxy for past water environments in polar regions. *Glob. Change Biol.* **21**, 2454–2464.

Brenninkmeijer C. A. M., van Geel B. and Mook W. G. (1982) Variations in the D/H and $^{18}O/^{16}O$ ratios in cellulose extracted from a peat bog core. *Earth Planet. Sci. Lett.* **61**, 283–290.

Chambers F. M., Booth R. K., De Vleeschouwer F., Lamentowicz M., Le Roux G., Mauquoy D., Nichols J. E. and van Geel B. (2012) Development and refinement of proxy-climate indicators from peats. *Quat. Int.* **268**, 21–33.

Charman D. J. (2007) Summer water deficit variability controls on peatland water-table changes: implications for Holocene palaeoclimate reconstructions. *Holocene* **17**, 217–227.

Clymo R. S. (1970) The growth of *Sphagnum*: methods of measurement. *J. Ecol.* **58**, 13–49.

Craig H. and Gordon L. I. (1965) Deuterium and oxygen 18 variations in the ocean and the marine atmosphere. In *Stable Isotopes in Oceanographic Studies and Paleotemperatures* (ed. E. Tongiorgi). Consiglio nazionale delle Ricerche Laboratorio di Geologia Nucleare, Spoleto, pp. 9–130.

Daley T. J., Street-Perrott F. A., Loader N. J., Barber K. E., Hughes P. D. M., Fisher E. H. and Marshall J. D. (2009) Terrestrial climate signal of the "8200 yr B.P. cold event" in the Labrador Sea region. *Geology* **37**, 831–834.

Daley T. J., Barber K. E., Street-Perrott F. A., Loader N. J., Marshall J. D., Crowley S. F. and Fisher E. H. (2010) Holocene climate variability revealed by oxygen isotope analysis of *Sphagnum* cellulose from Walton Moss, northern England. *Quat. Sci. Rev.* **29**, 1590–1601.

Daley T. J., Mauquoy D., Chambers F. M., Street-Perrott F. A., Hughes P. D. M., Loader N. J., Roland T. P., van Bellen S., Garcia-Meneses P. and Lewin S. (2012) Investigating late Holocene variations in hydroclimate and the stable isotope composition of precipitation using southern South American peatlands: an hypothesis. *Clim. Past* **8**, 1457–1471.

Daniels W. C., Russell J. M., Giblin A. E., Welker J. M., Klein E. S. and Huang Y. (2017) Hydrogen isotope fractionation in leaf waxes in the Alaskan Arctic tundra. *Geochim. Cosmochim. Acta* **213**, 216–236.

Dilks T. J. K. and Proctor M. C. F. (1979) Photosynthesis, respiration and water content in bryophytes. *New Phytol.* **82**, 97–114.

El Bilali H. and Patterson R. T. (2012) Influence of cellulose oxygen isotope variability in sub-fossil *Sphagnum* and plant macrofossil components on the reliability of paleoclimate records at the Mer Bleue Bog, Ottawa, Ontario, Canada. *Org. Geochem.* **43**, 39–49.

Farquhar G. D., Ehleringer J. R. and Hubick K. T. (1989) Carbon isotope discrimination and photosynthesis. *Annu. Rev. Plant Biol.* **40**, 503–537.

Finkenbinder M. S., Abbott M. B. and Steinman B. A. (2016) Holocene climate change in Newfoundland reconstructed using oxygen isotope analysis of lake sediment cores. *Glob. Planet. Chang.* **143**, 251–261.

Gonfiantini R. (1986) Environmental isotopes in lake studies. In *Handbook of Environmental Isotope Geochemistry, The Terrestrial Environment*, vol. 2 (eds. P. Fritz and J.-C. Fontes). Elsevier, Amsterdam, pp. 113–168.

Granath G., Rydin H., Baltzer J. L., Bengtsson F., Boncek N., Bragazza L., Bu Z. J., Caporn S. J. M., Dorrepaal E., Galanina O., Gałka M., Ganeva A., Gillikin D. P., Goia I., Goncharova N., Hájek M., Haraguchi A., Harris L. I., Humphreys E., Jiroušek M., Kajukało K., Karofeld E., Koronatova N. G., Kosykh N. P., Lamentowicz M., Lapshina E., Limpens J., Linkosalmi M., Ma J. Z., Mauritz M., Munir T. M., Natali S. M., Natcheva R., Noskova M., Payne R. J., Pilkington K., Robinson S., Robroek B. J. M., Rochefort L., Singer D., Stenøien H. K., Tuittila E. S., Vellak K., Verheyden A., Waddington J. M. and Rice S. K. (2018) Environmental and taxonomic controls of carbon and oxygen stable isotope composition in *Sphagnum* across broad climatic and geographic ranges. *Biogeosciences* **15**, 5189–5202.

Horita J. and Wesolowski D. J. (1994) Liquid-vapor fractionation of oxygen and hydrogen isotopes of water from the freezing to the critical temperature. *Geochim. Cosmochim. Acta* **58**, 3425–3437.

Kaislahti Tillman P., Holzkämper S., Kuhry P., Sannel A. B. K., Loader N. J. and Robertson I. (2010) Stable carbon and oxygen isotopes in *Sphagnum fuscum* peat from subarctic Canada: Implications for palaeoclimate studies. *Chem. Geol.* **270**, 216–226.

Kaislahti Tillman P., Holzkämper S., Andersen T. J., Hugelius G., Kuhry P. and Oksanen P. (2013) Stable isotopes in *Sphagnum fuscum* peat as late-Holocene climate proxies in northeastern European Russia. *Holocene* **23**, 1381–1390.

Lenaerts J. T. M., Broeke M. R. v. d., Wessem J. M. V., Berg W. J. V. D., Meijgaard E. V., Ulft L. H. V. and Schaefer M. (2014) Extreme precipitation and climate gradients in Patagonia revealed by high-resolution regional atmospheric climate modeling. *J. Clim.* **27**, 4607–4621.

Li G., Li L., Tarozo R., Longo W. M., Wang K. J., Dong H. and Huang Y. (2018) Microbial production of long-chain *n*-alkanes: Implication for interpreting sedimentary leaf wax signals. *Org. Geochem.* **115**, 24–31.

Loader N. J., McCarroll D., van der Knaap W. O., Robertson I. and Gagen M. (2007) Characterizing carbon isotopic variability in *Sphagnum*. *Holocene* **17**, 403–410.

Loader N. J., Street-Perrott F. A., Mauquoy D., Roland T. P., van Bellen S., Daley T. J., Davies D., Hughes P. D. M., Pancotto V. O., Young G. H. F., Amesbury M. J., Charman D. J., Mallon G. and Yu Z. C. (2016) Measurements of hydrogen, oxygen and carbon isotope variability in *Sphagnum* moss along a micro-topographical gradient in a southern Patagonian peatland. *J. Quatern. Sci.* **31**, 426–435.

Loisel J., Garneau M. and Hélie J. F. (2009) Modern *Sphagnum* $\delta^{13}C$ signatures follow a surface moisture gradient in two boreal peat bogs, James Bay lowlands, Québec. *J. Quatern. Sci.* **24**, 209–214.

Loisel J., Garneau M. and Hélie J.-F. (2010) *Sphagnum* $\delta^{13}C$ values as indicators of palaeohydrological changes in a peat bog. *Holocene* **20**, 285–291.

Loisel J., Gallego-Sala A. V. and Yu Z. (2012) Global-scale pattern of peatland *Sphagnum* growth driven by photosynthetically active radiation and growing season length. *Biogeosciences* **9**, 2737–2746.

Loisel J. and Yu Z. (2013a) Holocene peatland carbon dynamics in Patagonia. *Quat. Sci. Rev.* **69**, 125–141.

Loisel J. and Yu Z. (2013b) Surface vegetation patterning controls carbon accumulation in peatlands. *Geophys. Res. Lett.* **40**, 5508–5513.

Markel E. R., Booth R. K. and Qin Y. (2010) Testate amoebae and $\delta^{13}C$ of *Sphagnum* as surface-moisture proxies in Alaskan peatlands. *Holocene* **20**, 463–475.

Mayr C., Lücke A., Stichler W., Trimborn P., Ercolano B., Oliva G., Ohlendorf C., Soto J., Fey M., Haberzettl T., Janssen S., Schäbitz F., Schleser G. H., Wille M. and Zolitschka B. (2007) Precipitation origin and evaporation of lakes in semi-arid Patagonia (Argentina) inferred from stable isotopes ($\delta^{18}O$, $\delta^{2}H$). *J. Hydrol.* **334**, 53–63.

Ménot-Combes G., Burns S. J. and Leuenberger M. (2002) Variations of $^{18}O/^{16}O$ in plants from temperate peat bogs (Switzerland): implications for paleoclimatic studies. *Earth Planet. Sci. Lett.* **202**, 419–434.

Ménot G. and Burns S. J. (2001) Carbon isotopes in ombrogenic peat bog plants as climatic indicators: calibration from an altitudinal transect in Switzerland. *Org. Geochem.* **32**, 233–245.

Meyer M., Seibt U. and Griffiths H. (2008) To concentrate or ventilate? Carbon acquisition, isotope discrimination and physiological ecology of early land plant life forms. *Phil. Trans. R. Soc. B* **363**, 2767–2778.

Mora G. and Zanazzi A. (2017) Hydrogen isotope ratios of moss cellulose and source water in wetlands of Lake Superior, United States reveal their potential for quantitative paleoclimatic reconstructions. *Chem. Geol.* **468**, 75–83.

Moschen R., Kühl N., Rehberger I. and Lücke A. (2009) Stable carbon and oxygen isotopes in sub-fossil *Sphagnum*: Assessment of their applicability for palaeoclimatology. *Chem. Geol.* **259**, 262–272.

Moschen R., Kühl N., Peters S., Vos H. and Lücke A. (2011) Temperature variability at Dürres Maar, Germany during the Migration Period and at High Medieval Times, inferred from stable carbon isotopes of *Sphagnum* cellulose. *Clim. Past* **7**, 1011–1026.

Murray K. J., Harley P. C., Beyers J., Walz H. and Tenhunen J. D. (1989) Water content effects on photosynthetic response of *Sphagnum* mosses from the foothills of the Philip Smith Mountains, Alaska. *Oecologia* **79**, 244–250.

Nichols J., Booth R. K., Jackson S. T., Pendall E. G. and Huang Y. (2010) Differential hydrogen isotopic ratios of *Sphagnum* and vascular plant biomarkers in ombrotrophic peatlands as a quantitative proxy for precipitation—evaporation balance. *Geochim. Cosmochim. Acta* **74**, 1407–1416.

Nichols J. E., Booth R. K., Jackson S. T., Pendall E. G. and Huang Y. (2006) Paleohydrologic reconstruction based on *n*-alkane distributions in ombrotrophic peat. *Org. Geochem.* **37**, 1505–1513.

Nichols J. E., Walcott M., Bradley R., Pilcher J. and Huang Y. (2009) Quantitative assessment of precipitation seasonality and summer surface wetness using ombrotrophic sediments from an Arctic Norwegian peatland. *Quat. Res.* **72**, 443–451.

Nichols J. E., Isles P. D. F. and Peteet D. M. (2014) A novel framework for quantifying past methane recycling by *Sphagnum*-methanotroph symbiosis using carbon and hydrogen isotope ratios of leaf wax biomarkers. *Geochem. Geophys. Geosys.* **15**, 1827–1836.

Pendall E., Markgraf V., White J. W. C., Dreier M. and Kenny R. (2001) Multiproxy record of late Pleistocene-Holocene climate and vegetation changes from a peat bog in Patagonia. *Quat. Res.* **55**, 168–178.

Price G. D., McKenzie J. E., Pilcher J. R. and Hoper S. T. (1997) Carbon-isotope variation in *Sphagnum* from hummock-hollow complexes: implications for Holocene climate reconstruction. *Holocene* **7**, 229–233.

Price J. S., Edwards T. W. D., Yi Y. and Whittington P. N. (2009) Physical and isotopic characterization of evaporation from *Sphagnum* moss. *J. Hydrol.* **369**, 175–182.

Proctor M. C. F., Raven J. A. and Rice S. K. (1992) Stable carbon isotope discrimination measurements in *Sphagnum* and other bryophytes: physiological and ecological implications. *J. Bryol.* **17**, 193–202.

Proctor M. C. F., Nagy Z., Csintalan Z. and Takács Z. (1998) Water-content components in bryophytes: analysis of pressure-volume relationships. *J. Exp. Bot.* **49**, 1845–1854.

Raghoebarsing A. A., Smolders A. J. P., Schmid M. C., Rijpstra W. I. C., Wolters-Arts M., Derksen J., Jetten M. S. M., Schouten S., Sinninghe Damsté J. S., Lamers L. P. M., Roelofs J. G. M., Op den Camp H. J. M. and Strous M. (2005) Methanotrophic symbionts provide carbon for photosynthesis in peat bogs. *Nature* **436**, 1153–1156.

Rice S. K. and Giles L. (1996) The influence of water content and leaf anatomy on carbon isotope discrimination and photosynthesis in *Sphagnum*. *Plant Cell Environ.* **19**, 118–124.

Rice S. K. (2000) Variation in carbon isotope discrimination within and among *Sphagnum* species in a temperate wetland. *Oecologia* **123**, 1–8.

Roland T. P., Daley T. J., Caseldine C. J., Charman D. J., Turney C. S. M., Amesbury M. J., Thompson G. J. and Woodley E. J. (2015) The 5.2 ka climate event: Evidence from stable isotope and multi-proxy palaeoecological peatland records in Ireland. *Quat. Sci. Rev.* **124**, 209–223.

Royles J., Ogée J., Wingate L., Hodgson D. A., Convey P. and Griffiths H. (2012) Carbon isotope evidence for recent climate-related enhancement of CO_2 assimilation and peat accumulation rates in Antarctica. *Glob. Change Biol.* **18**, 3112–3124.

Royles J., Ogée J., Wingate L., Hodgson D. A., Convey P. and Griffiths H. (2013a) Temporal separation between CO_2 assimilation and growth? Experimental and theoretical evidence from the desiccation-tolerant moss *Syntrichia ruralis*. *New Phytol.* **197**, 1152–1160.

Royles J., Sime L. C., Hodgson D. A., Convey P. and Griffiths H. (2013b) Differing source water inputs, moderated by evaporative enrichment, determine the contrasting $\delta^{18}O_{CELLULOSE}$ signals in maritime Antarctic moss peat banks. *J. Geophys. Res. Biogeo.* **118**, 184–194.

Royles J. and Griffiths H. (2015) Invited review: climate change impacts in polar regions: lessons from Antarctic moss bank archives. *Glob. Change Biol.* **21**, 1041–1057.

Royles J., Amesbury M. J., Roland T. P., Jones G. D., Convey P., Griffiths H., Hodgson D. A. and Charman D. J. (2016) Moss stable isotopes (carbon-13, oxygen-18) and testate amoebae reflect environmental inputs and microclimate along a latitudinal gradient on the Antarctic Peninsula. *Oecologia* **181**, 931–945.

Rydin H. and McDonald A. J. S. (1985) Photosynthesis in *Sphagnum* at different water contents. *J. Bryol.* **13**, 579–584.

Rydin H. and Jeglum J. K. (2013) *The Biology of Peatlands*, second ed. Oxford University Press, Oxford, UK.

Sachse D., Billault I., Bowen G. J., Chikaraishi Y., Dawson T. E., Feakins S. J., Freeman K. H., Magill C. R., McInerney F. A., Meer M. T. J. v. d., Polissar P., Robins R. J., Sachs J. P., Schmidt H.-L., Sessions A. L., White J. W. C., West J. B. and Kahmen A. (2012) Molecular paleohydrology: interpreting the hydrogen-isotopic composition of lipid biomarkers from photosynthesizing organisms. *Annu. Rev. Earth Planet. Sci.* **40**, 221–249.

Schipperges B. and Rydin H. (1998) Response of photosynthesis of *Sphagnum* species from contrasting microhabitats to tissue water content and repeated desiccation. *New Phytol.* **140**, 677–684.

Sessions A. L., Burgoyne T. W., Schimmelmann A. and Hayes J. M. (1999) Fractionation of hydrogen isotopes in lipid biosynthesis. *Org. Geochem.* **30**, 1193–1200.

Silvola J. and Aaltonen H. (1984) Water content and photosynthesis in the peat mosses Sphagnum fuscum and S. angustifolium. *Annales Botanici Fennici* **21**, 1–6.

Skrzypek G., Kałużny A., Wojtuń B. and Jędrysek M.-O. (2007) The carbon stable isotopic composition of mosses: A record of temperature variation. *Org. Geochem.* **38**, 1770–1781.

Smart R. E. and Bingham G. E. (1974) Rapid estimates of relative water content. *Plant Physiol.* **53**, 258–260.

Sobotka D. (1976) Regeneration and vegetative propagation of *Sphagnum palustre* as factor of population stability. *Acta Societatis Botanicorum Poloniae* **45**, 357–368.

Sternberg L. and Ellsworth P. F. V. (2011) Divergent biochemical fractionation, not convergent temperature, explains cellulose oxygen isotope enrichment across latitudes. *PloS ONE* **6**, e28040.

Sternberg L. D. S. L., Deniro M. J. and Savidge R. A. (1986) Oxygen isotope exchange between metabolites and water during biochemical reactions leading to cellulose synthesis. *Plant Physiol.* **82**, 423–427.

Sternberg L. S. L. (2009) Oxygen stable isotope ratios of tree-ring cellulose: the next phase of understanding. *New Phytol.* **181**, 553–562.

Stokes J. R., Alspach P. A. and Stanley C. J. (1999) Effect of water table on growth of three New Zealand *Sphagnum* species: implications for *S. cristatum* management. *J. Bryol.* **21**, 25–29.

Swindles G. T., Morris P. J., Baird A. J., Blaauw M. and Plunkett G. (2012) Ecohydrological feedbacks confound peat-based climate reconstructions. *Geophys. Res. Lett.* **39**, L11401.

Titus J. E., Wagner D. J. and Stephens M. D. (1983) Contrasting water relations of photosynthesis for two *Sphagnum* mosses. *Ecology* **64**, 1109–1115.

Titus J. E. and Wagner D. J. (1984) Carbon balance for two *Sphagnum* mosses: water balance resolves a physiological paradox. *Ecology* **65**, 1765–1774.

Turetsky M. R., Crow S. E., Evans R. J., Vitt D. H. and Wieder R. K. (2008) Trade-offs in resource allocation among moss species control decomposition in boreal peatlands. *J. Ecol.* **96**, 1297–1305.

Turney C. S. M., Kershaw A. P., Clemens S. C., Branch N., Moss P. T. and Keith Fifield L. (2004) Millennial and orbital variations of El Niño/Southern Oscillation and high-latitude climate in the last glacial period. *Nature* **428**, 306–310.

Van Bellen S., Mauquoy D., Payne R. J., Roland T. P., Daley T. J., Hughes P. D. M., Loader N. J., Street-perrott F. A., Rice E. M. and Pancotto V. A. (2014) Testate amoebae as a proxy for reconstructing Holocene water table dynamics in southern Patagonian peat bogs. *J. Quatern. Sci.* **29**, 463–474.

Williams T. G. and Flanagan L. B. (1996) Effect of changes in water content on photosynthesis, transpiration and discrimination against $^{13}CO_2$ and $C^{18}O^{16}O$ in *Pleurozium* and *Sphagnum*. *Oecologia* **108**, 38–46.

Woodland W. A., Charman D. J. and Sims P. C. (1998) Quantitative estimates of water tables and soil moisture in Holocene peatlands from testate amoebae. *Holocene* **8**, 261–273.

Xia Z., Yu Z. and Loisel J. (2018) Centennial-scale dynamics of the Southern Hemisphere Westerly Winds across the Drake Passage over the past two millennia. *Geology* **46**, 855–858.

Xie S., Nott C. J., Avsejs L. A., Volders F., Maddy D., Chambers F. M., Gledhill A., Carter J. F. and Evershed R. P. (2000) Palaeoclimate records in compound-specific δD values of a lipid biomarker in ombrotrophic peat. *Org. Geochem.* **31**, 1053–1057.

Xie S., Nott C. J., Avsejs L. A., Maddy D., Chambers F. M. and Evershed R. P. (2004) Molecular and isotopic stratigraphy in an ombrotrophic mire for paleoclimate reconstruction. *Geochim. Cosmochim. Acta* **68**, 2849–2862.

Yakir D. (1992) Variations in the natural abundance of oxygen-18 and deuterium in plant carbohydrates. *Plant Cell Environ.* **15**, 1005–1020.

Yu Z., Loisel J., Brosseau D. P., Beilman D. W. and Hunt S. J. (2010) Global peatland dynamics since the Last Glacial Maximum. *Geophys. Res. Lett.* **37**, L13402.

Zanazzi A. and Mora G. (2005) Paleoclimatic implications of the relationship between oxygen isotope ratios of moss cellulose and source water in wetlands of Lake Superior. *Chem. Geol.* **222**, 281–291.

Zech M., Mayr C., Tuthorn M., Leiber-Sauheitl K. and Glaser B. (2014) Oxygen isotope ratios ($^{18}O/^{16}O$) of hemicellulose-derived sugar biomarkers in plants, soils and sediments as paleoclimate proxy I: Insight from a climate chamber experiment. *Geochim. Cosmochim. Acta* **126**, 614–623.

Associate editor: Thomas Wagner